Atomic Data for Opacity Calculations

Jianmin Yuan

National University of Defense Technology
Department of Physics
Changsha 410073, China

Meudon, Oct.19,2006

Outline

1. Introduction
2. The physics model and atomic data
3. Results and discussion
4. Conclusion

Introduction

- Opacity calculation concerns a variety of atomic data
- Opacity calculation requires huge number of atomic data
- Opacity calculation involves various approximate treatments
- What accuracy does opacity calculation require for atomic data?

2. The physics model

1. Detailed-term-accounting or Detailed-level-accounting treatment for bound-bound and bound-free processes
2. SCF, MCSCF, and CI are used for the calculation of energy levels and oscillator strength
3. BF process: one-configuration and multi-channel (close-coupling)
4. Line broadening: semi-classical and full quantum mechanical（impact approximation）
5. Occupations: Saha equation (low density)，average atom (AA) model (high density), others?

2. The physics model (continued)

The opacity can be written in terms of

$$K_\nu = \frac{N_A}{A}\left[\sigma^{bb}(h\nu) + \sigma^{bf}(h\nu) + \sigma^{ff}(h\nu)\right]\times$$

$$\times\left(1 - e^{-h\nu/kT}\right) + K_{sc}$$

Where N_A is the Avogadro constant, A, the atomic weight, k, the Boltzmann constant, and σ, the cross sections of the optical transitions.

2. The physics model (continued)

For bound-bound transitions

$$\sigma_{i,j}^{bb}(h\nu) = \frac{2\pi^2}{c} f_{i,j}(h\nu)\varphi_{i,j}(h\nu)$$

Where f_{ij} is the oscillator strength, and φ_{ij}, the line profile. For the bound-free process

$$\sigma_{i,\varepsilon}^{bf}(h\nu) = \frac{2\pi^2}{c}\frac{df_{i,\varepsilon}(h\nu)}{d(h\nu)}$$

and df/dε is the density of the oscillator strength.

2. The physics model (continued)

For the free-free process, the Kramers formula is used to make a statistical average over the free electron distribution

$$\sigma^{ff}(h\nu) = \frac{32\pi^{5/2} Z^{*3} N_{ion}}{3\sqrt{6}c(kT)^{1/2}(h\nu)^3} g_{ff}(h\nu)$$

Where Z^* is the average ionization, N_{ion}, the number density of the ions, g_{ff}, the Gaunt factor.

2. The physics model (continued)

In hot and dense plasma, the line broadening are mainly due to the Doppler and Stark effects. Autoionization is also an important factor to be considered for line profiles. The Doppler profile has the form

$$\varphi_{i,j}^{Doppler}(h\nu) = \left(\frac{1}{2\pi\Delta^2}\right)^{\frac{1}{2}} e^{-\frac{(h\nu - h\nu_0)^2}{2\Delta^2}}$$

$$h\nu_0 = \varepsilon_j - \varepsilon_i$$

2. The physics model (continued)

Electron impact induced Lorentz profile：

$$\varphi_{i,j}^{impact}(h\nu) = \frac{\gamma}{\pi[(h\nu + \chi - h\nu_0)^2 + \gamma^2]}$$

$$h\nu_0 = \varepsilon_j - \varepsilon_i$$

Where γ and χ are：

$$\gamma + i\chi = N_e \frac{\hbar^2}{m}\left(\frac{2\pi}{mkT}\right)^{\frac{1}{2}} Y_D(T)$$

2. The physics model (continued)

Y_D is the thermal average collision strength :

$$Y_D(T) = \int_0^\infty \Omega_D(\varepsilon) e^{-\varepsilon/kT} d(\varepsilon/kT)$$

$$\Omega_D(\varepsilon) = (2S_A+1)^{-1} \sum_S \sum_{L\pi} \sum_{L'\pi'} \sum_{ll'} (2S+1)(2L+1)(2L'+1) \times$$

$$\times W(L_i L_j LL';1l) W L_i L_j LL';1l') \times$$

$$\times [\delta(ll') - S_i(SL\pi, ll') * S_j(SL'\pi', ll')]$$

Where ε is the electron energy, S_i, S_j are the elastic electron scattering matrix elements, respectively, for the initial and final states for the optical transition.

2. The physics model (continued)

$$\Gamma_l = N_e \frac{8\pi^2}{3\sqrt{3}} \frac{\hbar^2}{m^2} \left(\frac{2m}{\pi kT}\right)^{1/2} [R^2_{l_i,l_i+1} \tilde{g}\left(\frac{E}{\Delta E_{l_i,l_i+1}}\right) + R^2_{l_i,l_i-1} \tilde{g}\left(\frac{E}{\Delta E_{l_i,l_i-1}}\right) + R^2_{l_f,l_f+1} \tilde{g}\left(\frac{E}{\Delta E_{l_f,l_f+1}}\right)$$

$$+ R^2_{l_f,l_f-1} \tilde{g}\left(\frac{E}{\Delta E_{l_f,l_f-1}}\right) + \sum_{i'} (R^2_{ii'})_{\Delta n\neq 0}\, g\left(\frac{3kTn_i^3}{4z^2 E_H}\right) + \sum_{f'} (R^2_{ff'})_{\Delta n\neq 0}\, g\left(\frac{3kTn_f^3}{4z^2 E_H}\right)$$

$$\Gamma_l = N_e \frac{8\pi^2}{3\sqrt{3}} \frac{\hbar^3}{m^2} \left(\frac{2m}{\pi kT}\right)^{1/2} \left(0.9 - \frac{1.1}{z}\right) \sum_{j=i,f} \left(\frac{3n_j}{2z}\right)^2 (n_j^{\ 2} - l_j^{\ 2} - l_j - 1)$$

- The Doppler, electron impact, and the autoionizing broadening are taken into account.

3. Results and discussions

1. Line broadening by electron impact
2. Autoionization states
3. The x-ray transmission spectra of Al plasma:comparison with experiment
4. The spectral resolved opacities of Fe plasma
5. Br plasma opacity
6. Au plasma opacity

1. Spectra line broadening by electron impact

Lithium resonance line 2s ^2S–2p $^2P^o$:
Electron impact broadening (FWHW Width and shift) vs temperature (K) (electron density $10^{17}/cm^3$).
Conclusion: Considerable discrepancies are found between the quantum mechanical calculations and semiclassical treatment.

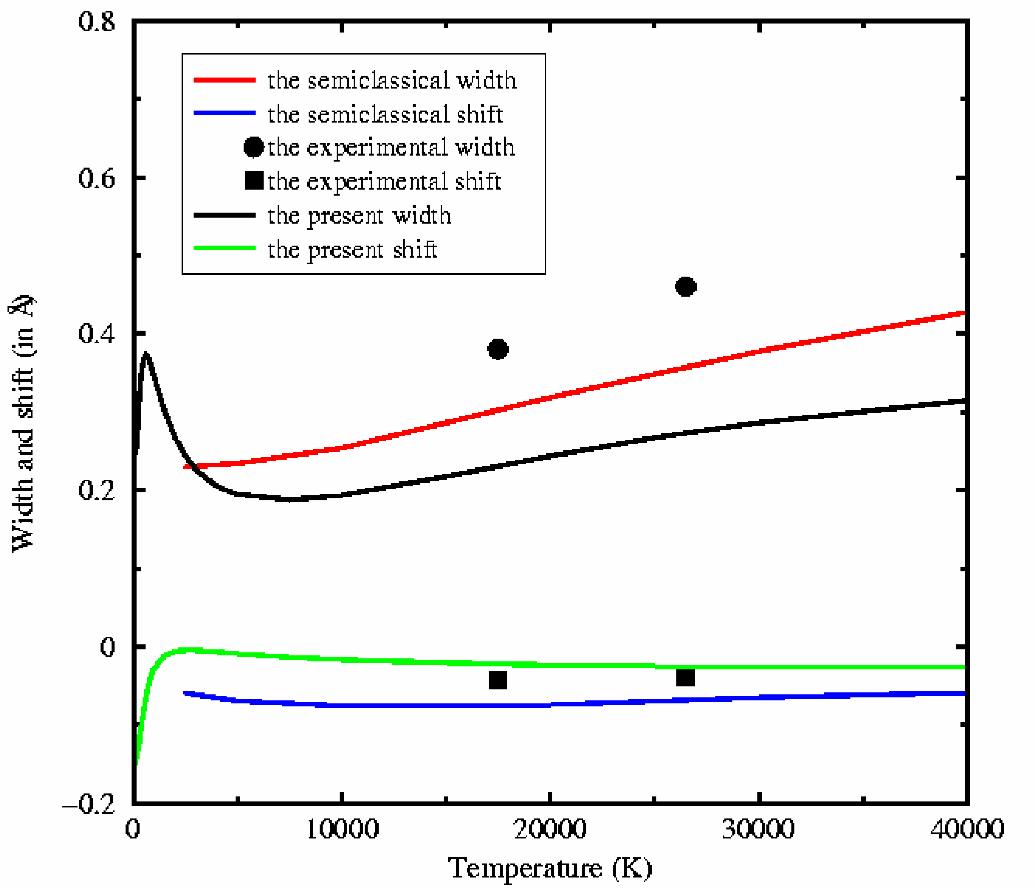

Chinese Phys. Letters **16**, 885(1999)

1. Spectra line broadening by electron impact(continued)

A quantum mechanical calculation

强激光与粒子束
High Power Laser and Particle Beam **13**, 60 (2001)

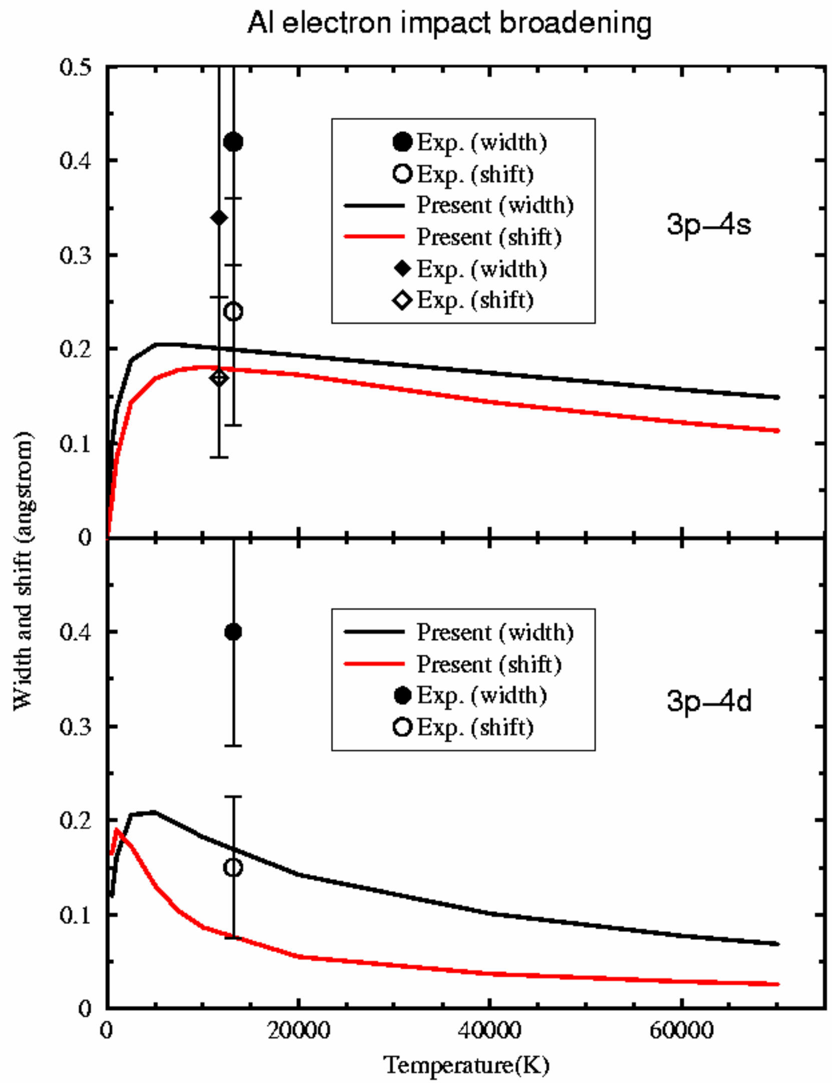

1. Spectra line broadening by electron impact(continued)

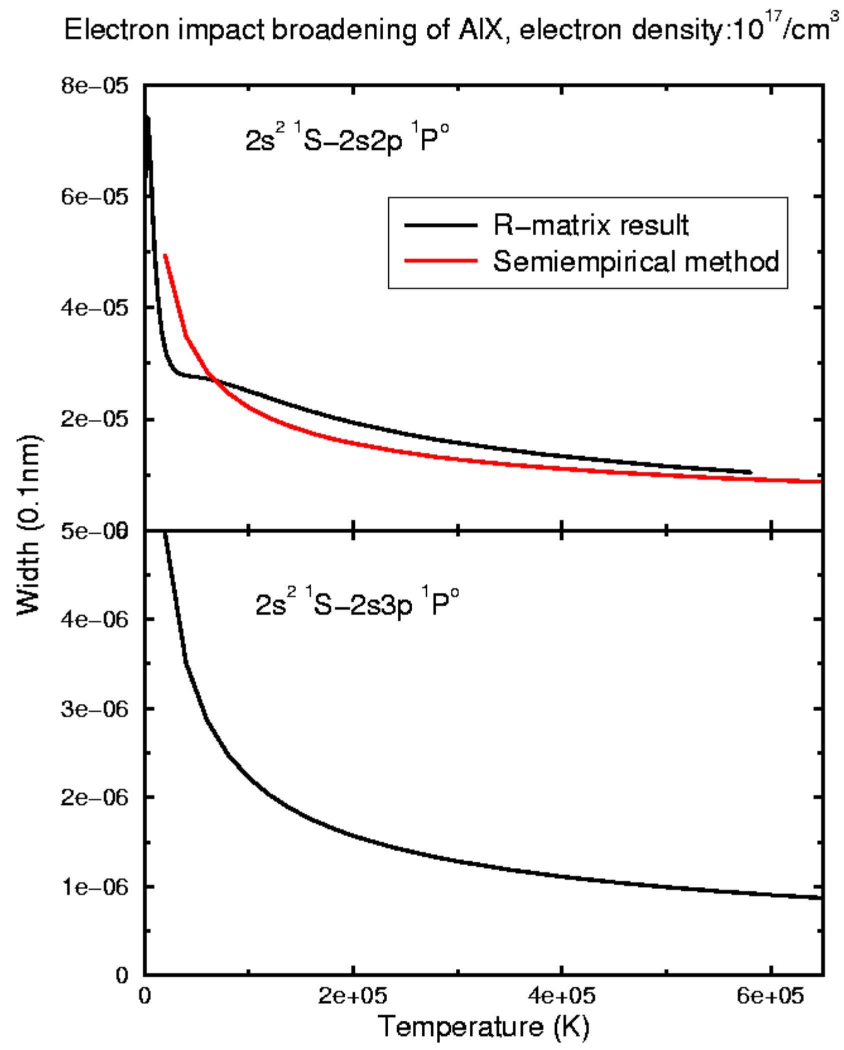

1. Spectra line broadening by electron impact(continued)

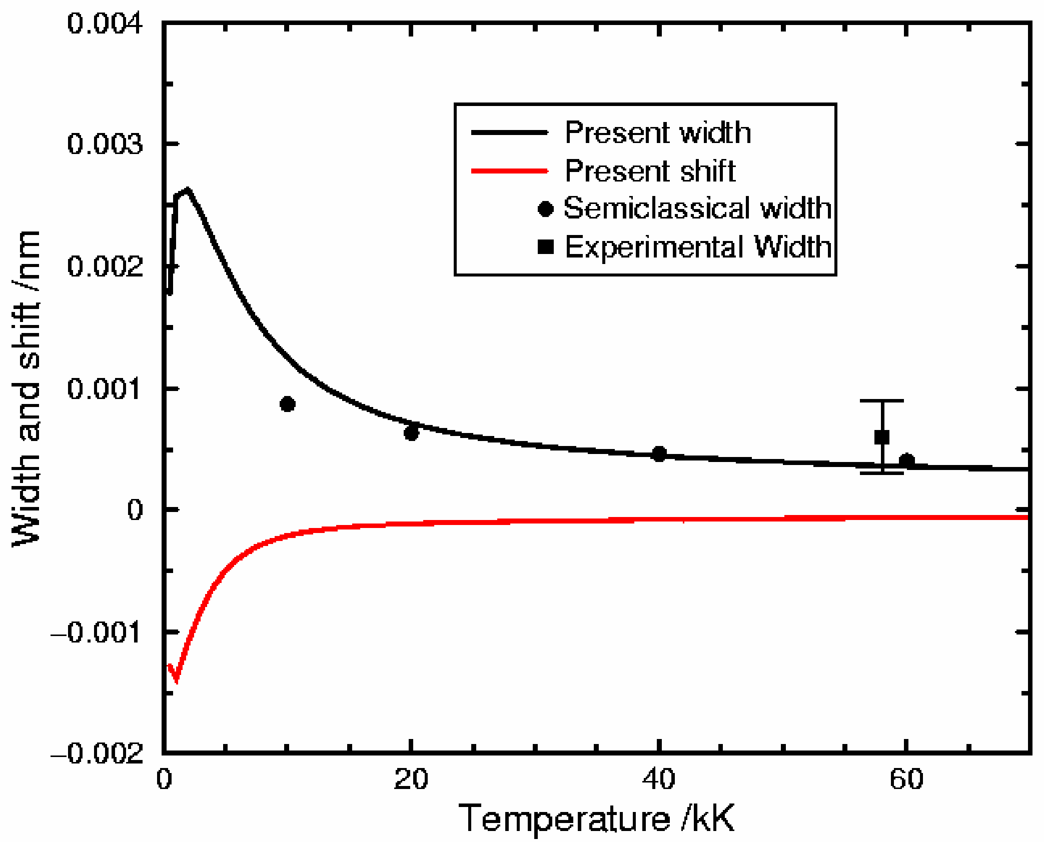

Electron impact broadening of C IV 2s–2p vs temperature
Electron density is taken as $10^{17}/cm^3$.

2. Autoionization lines

AlVIII photoabsorption cross section (in Mb) of the ground state

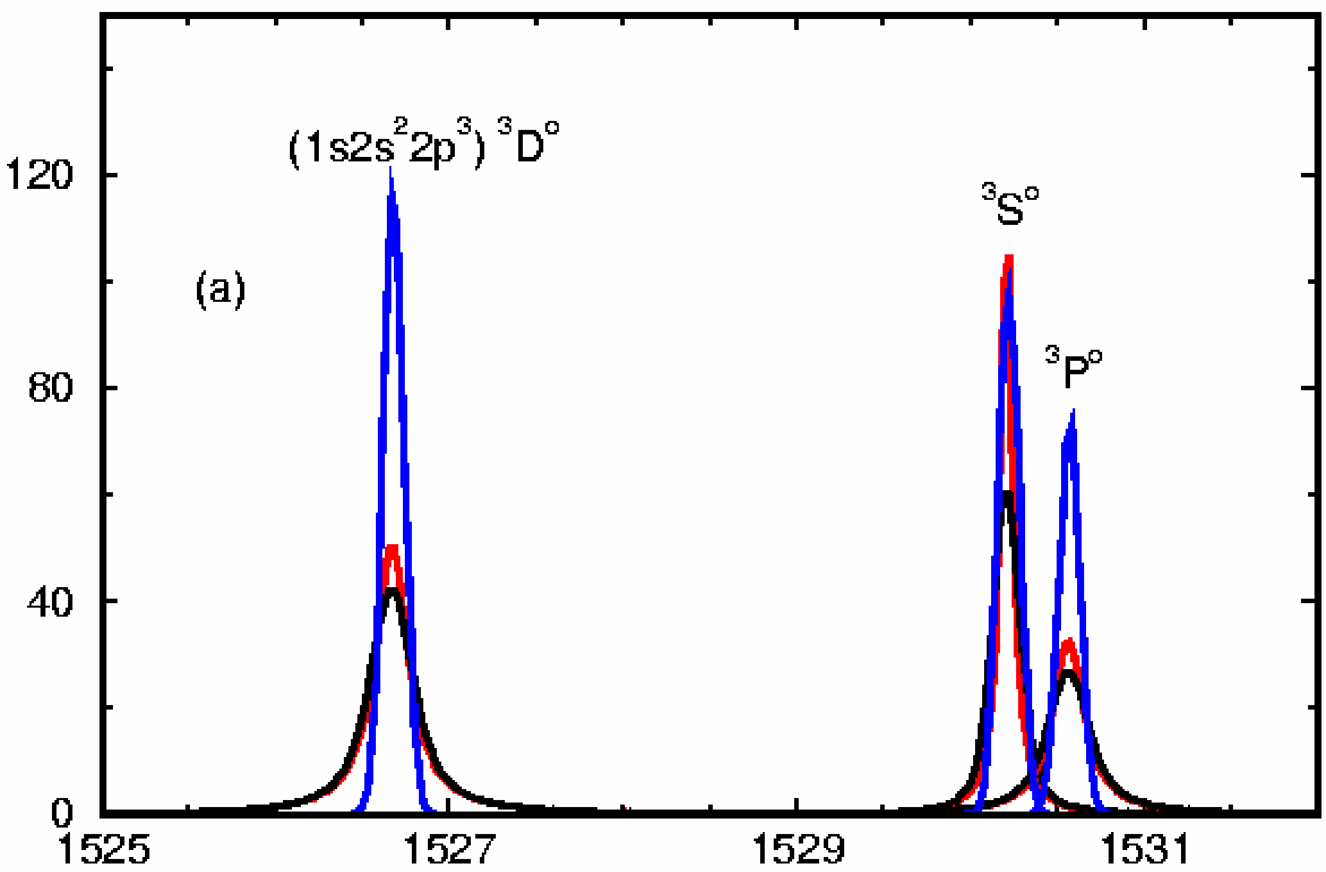

2. Autoionization lines (continued)

AlVIII photoabsorption cross section (in Mb) : sum of 12 low-lying states

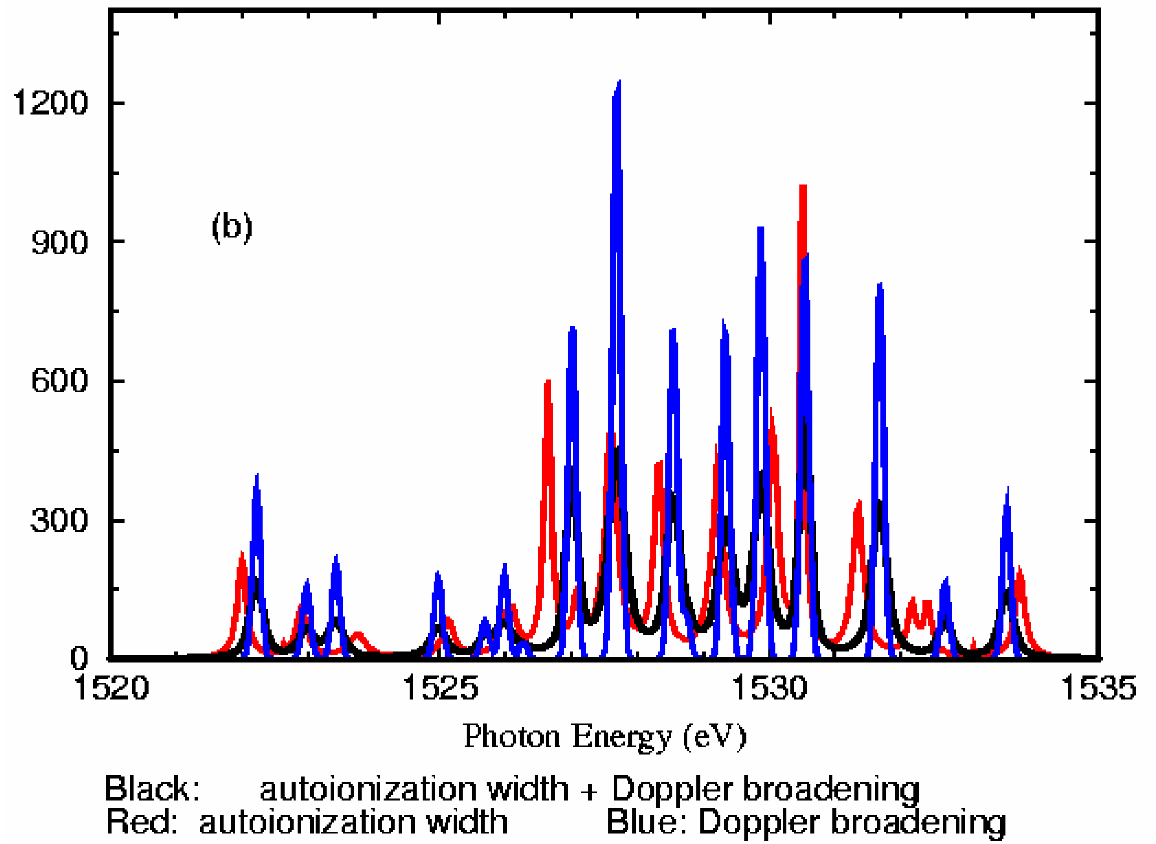

Phys. Rev. E **62**, 7251 (2000)

2. Autoionization lines (continued)

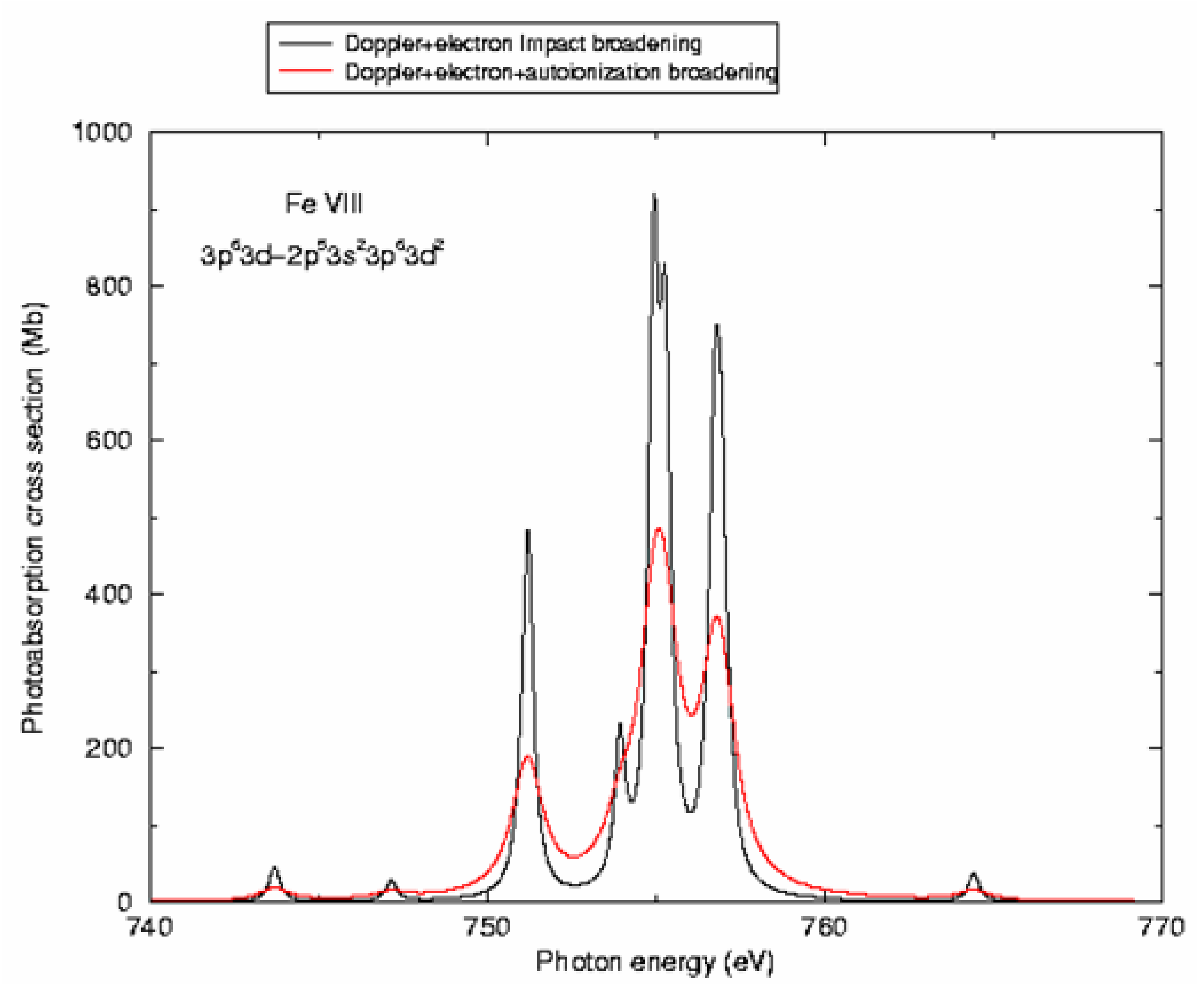

3. The x-ray transmission spectra of Al plasma: autoionization broadening

Phys. Rev. E **62**, 7251 (2000)

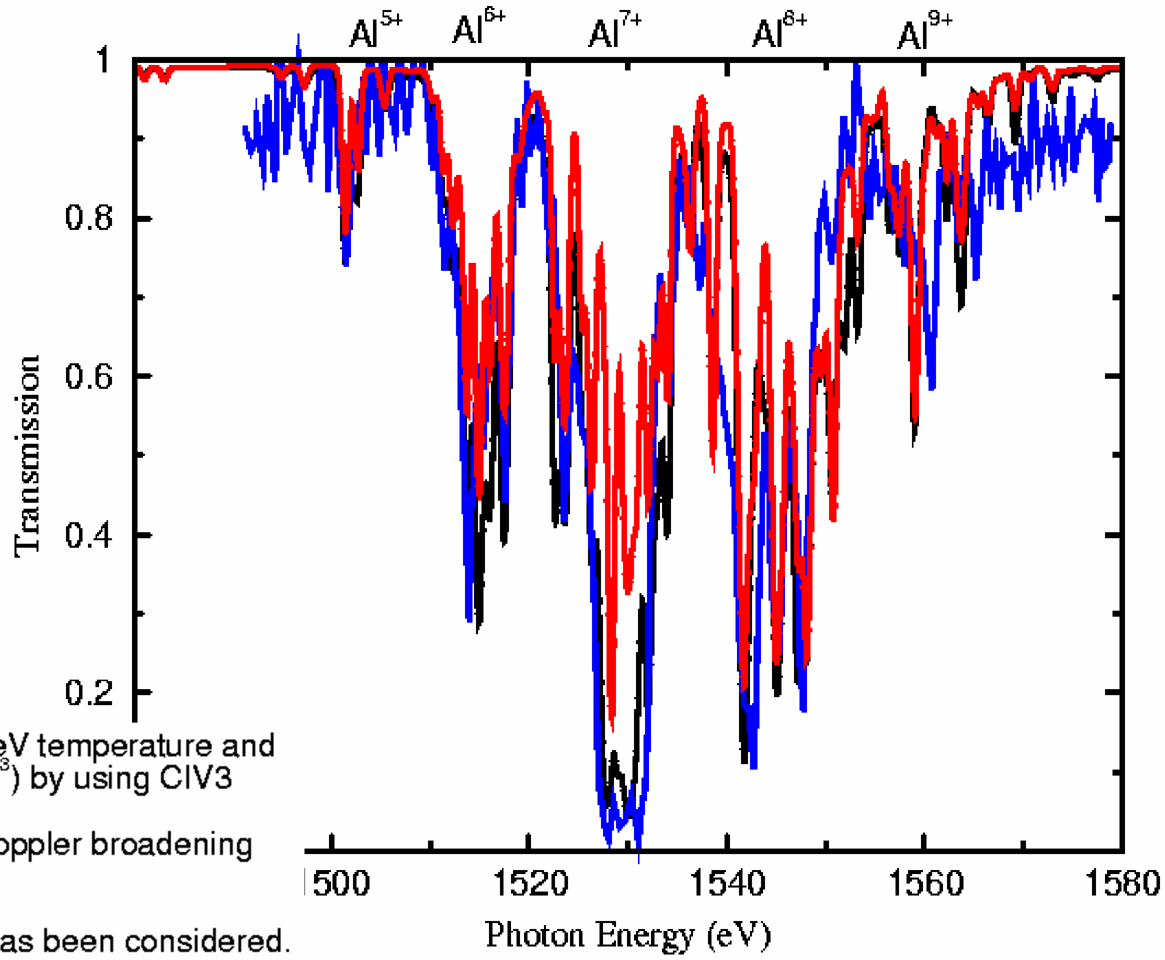

Transmission of Al Plasma: 40 eV temperature and 0.005 solid density (0.0135g/cm^3) by using CIV3 atomic structure code.
Black: autoionizayion width + Doppler broadening
Red: Doppler broadening
Blue: Experimental spectrum
Instrumental resolution 0.7 eV has been considered.

3. The x-ray transmission spectra of Al plasma: comparison with experiment (continued)

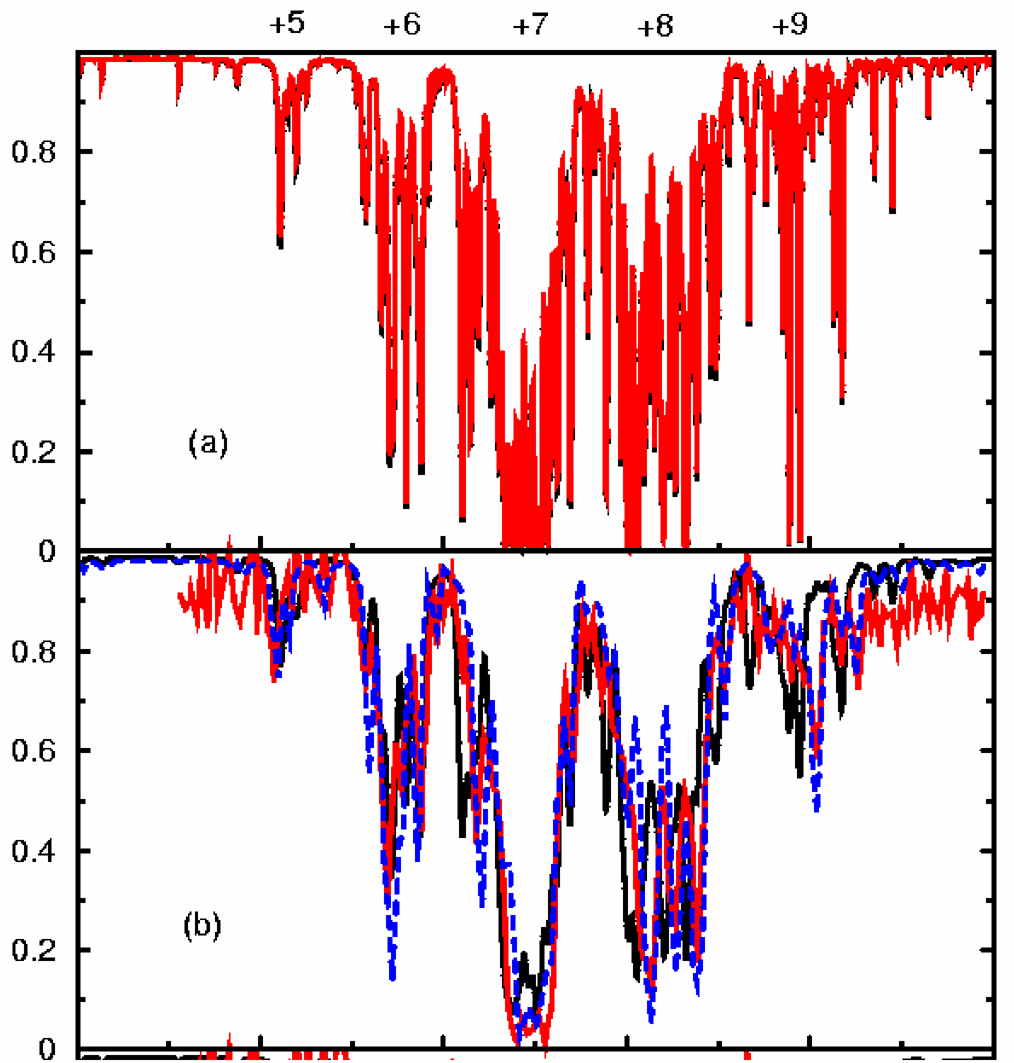

unconvoluted (a)

And

Convoluted (b)

3.The x-ray transmission spectra of Al plasma: autoionization broadening

An R-matrix calculation

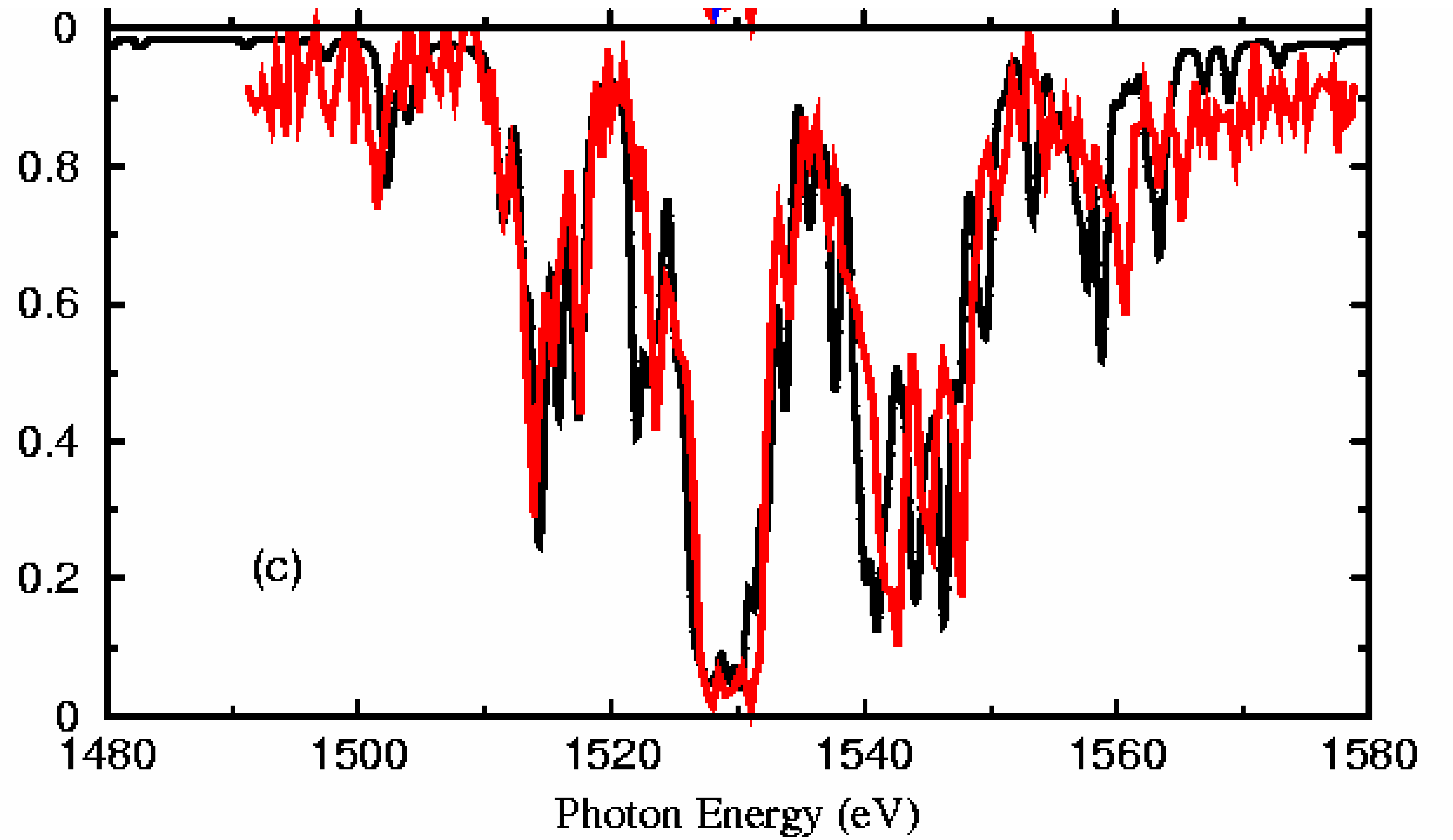

Davidson *et al*, APL. 52, 847 (1988). **Phys. Rev. E 62, 7251(2000)**

3. The x-ray transmission spectra of Al plasma: the relativistic effect

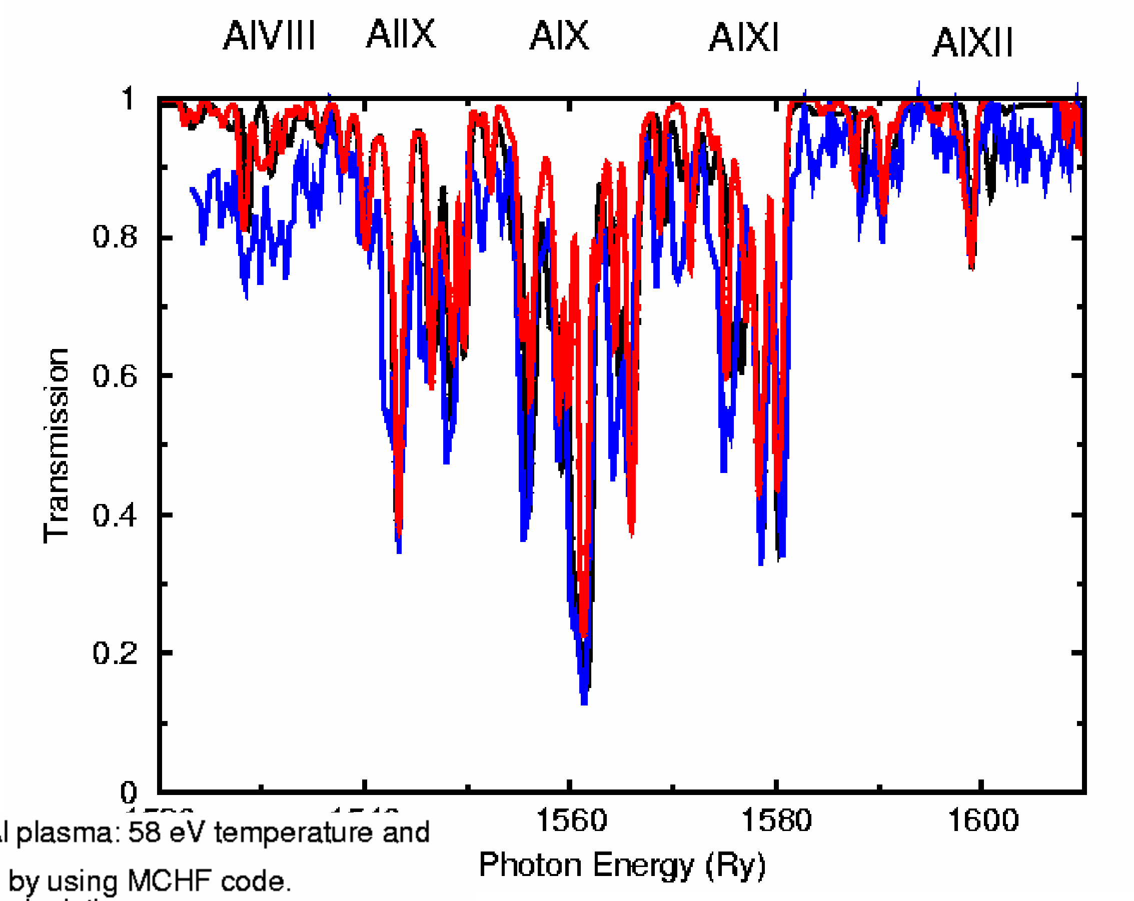

Transmission of Al plasma: 58 eV temperature and $0.02 g/cm^3$ density by using MCHF code.
Black: relativistic calculation
Red: non–relativistic calculation
Blue: Experimental spectrum

Instrumental resolution 0.6 eV has been considered.

Phys. Rev. E 62, 7251(2000)

3. The x-ray transmission spectra of Al plasma:
comparison with experiment(continued)

An R-matrix calculation

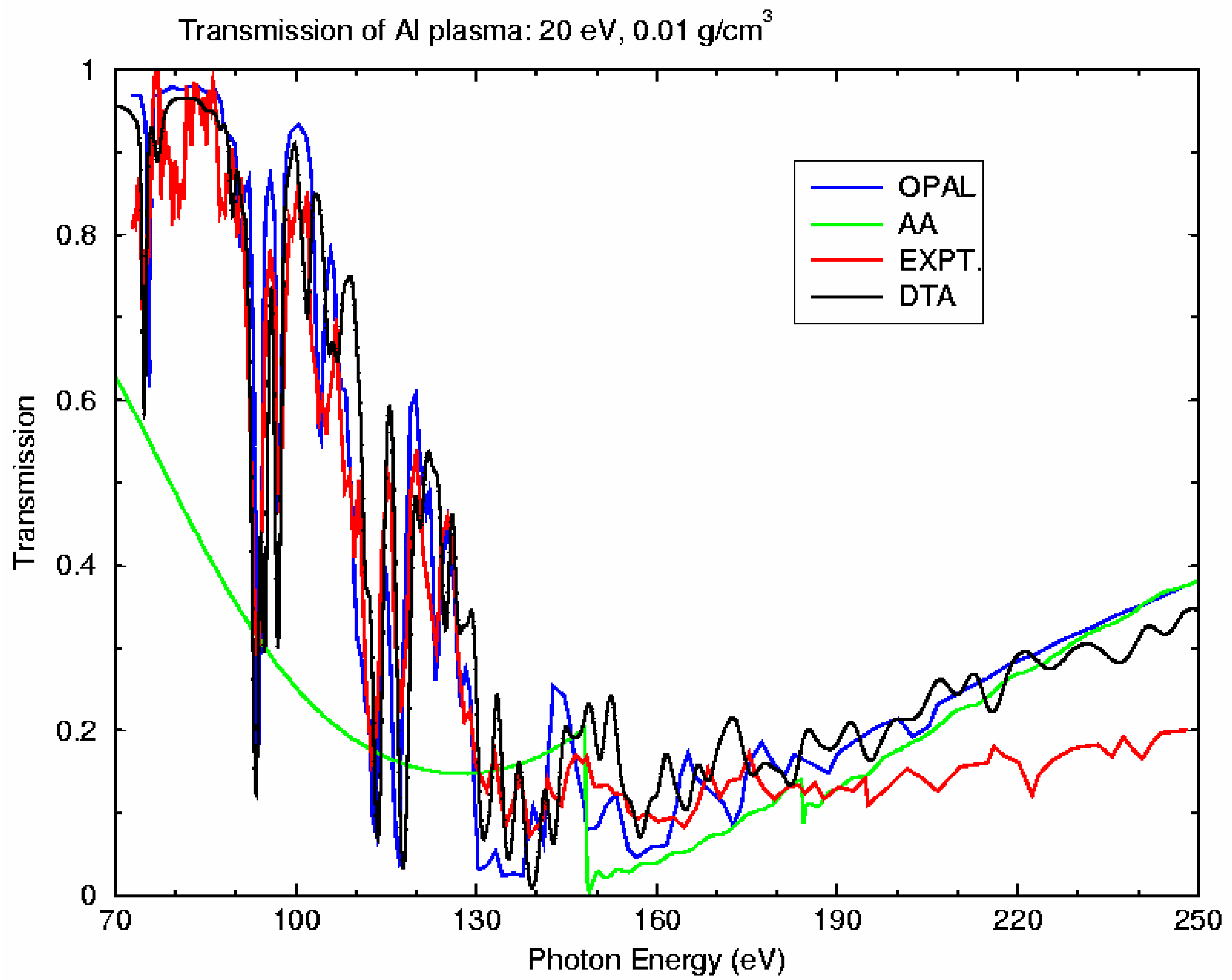

Phys. Rev. E 66, 016401 (2002) .

4. The spectra resolved and the mean opacity of Fe plasma

Winhart G *et al* 1996
Phys. Rev. E 53 R1332

$D=10^{-2}g/cm^3$

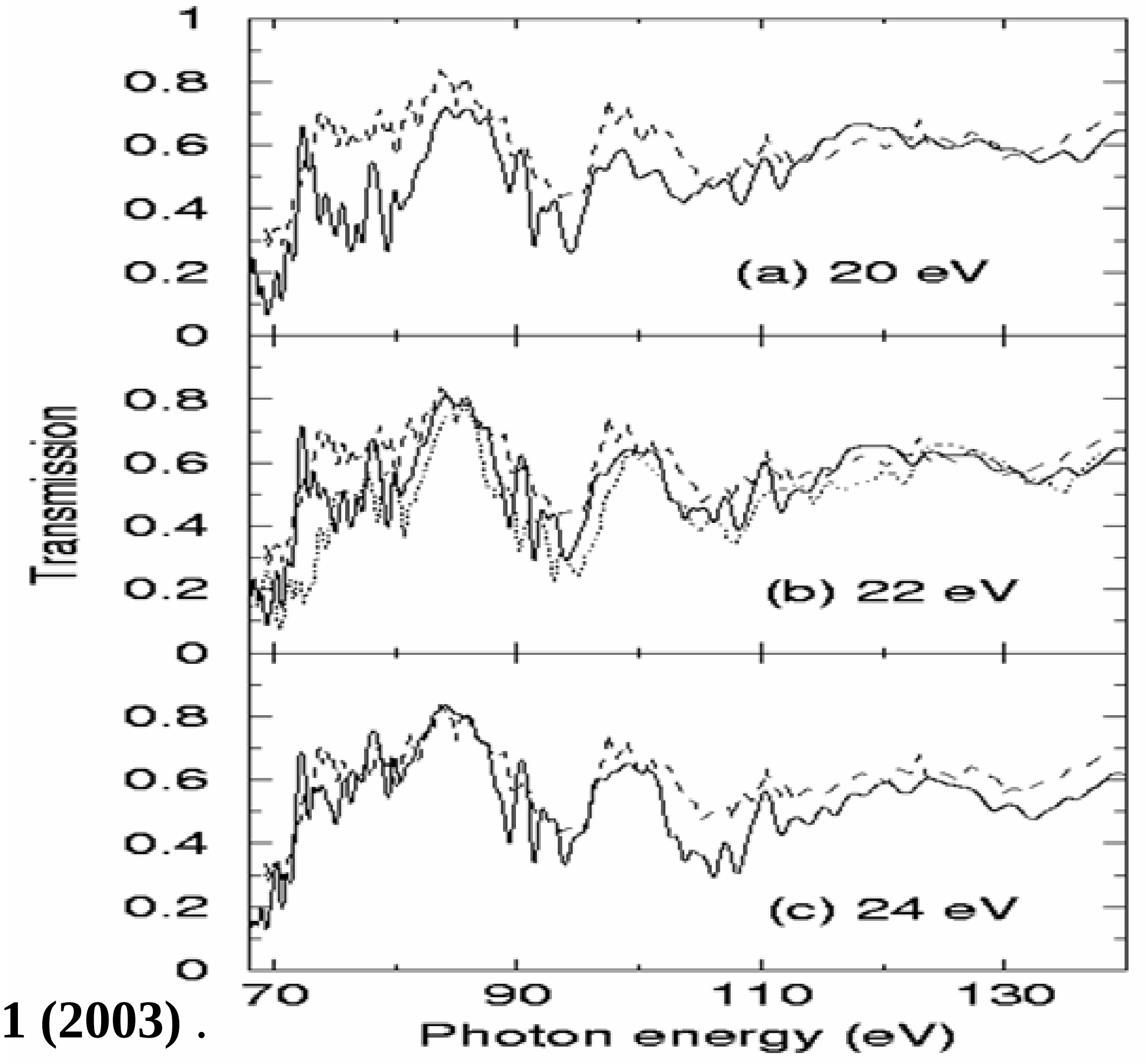

Phys. Rev. E 68, 066401 (2003) .

4. The spectra resolved and the mean opacity of Fe plasma (continued)

T=20eV

D=10^{-4}g/cm^3

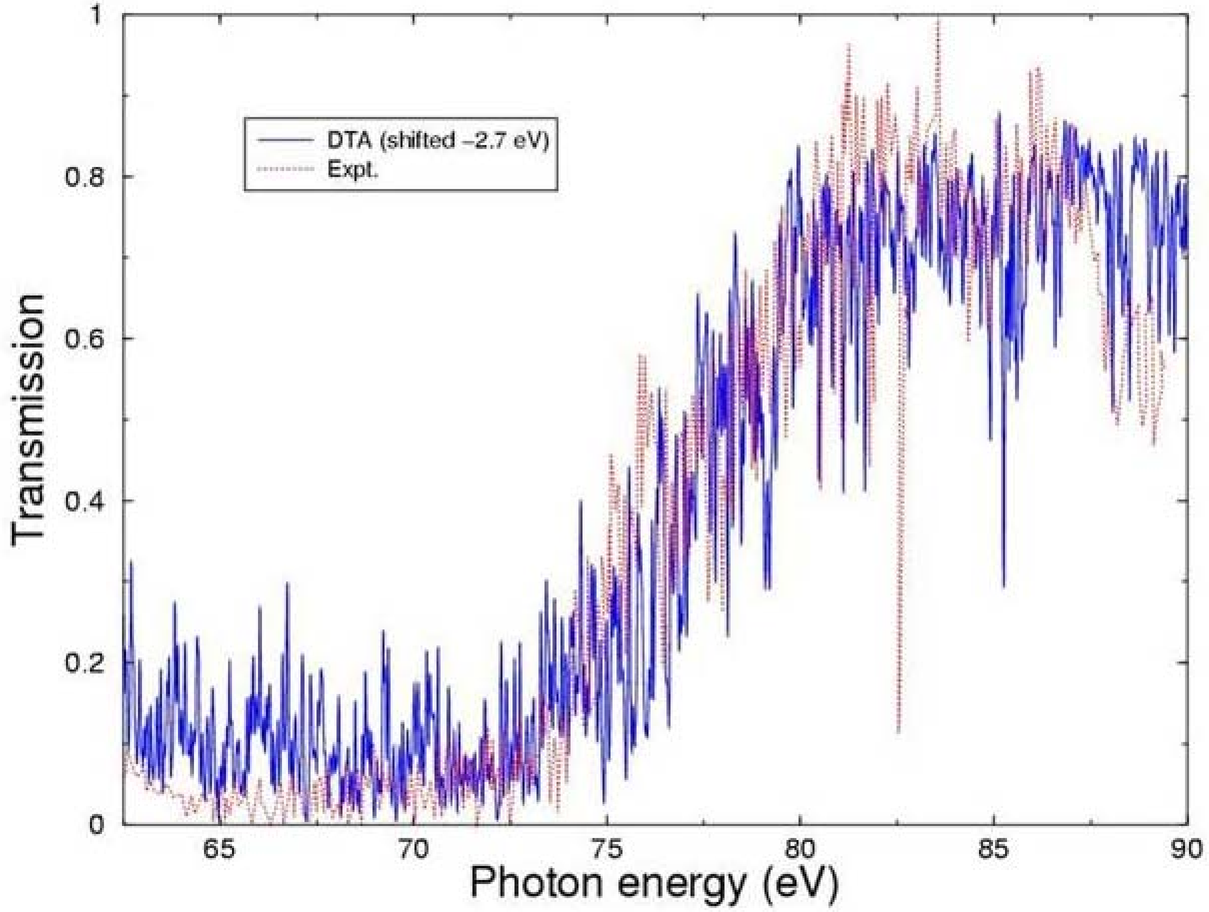

Phys. Rev. E 68, 066401 (2003) .

4. The spectra resolved and the mean opacity of Fe plasma (continued)

T=22eV

D=10^{-2}g/cm^3

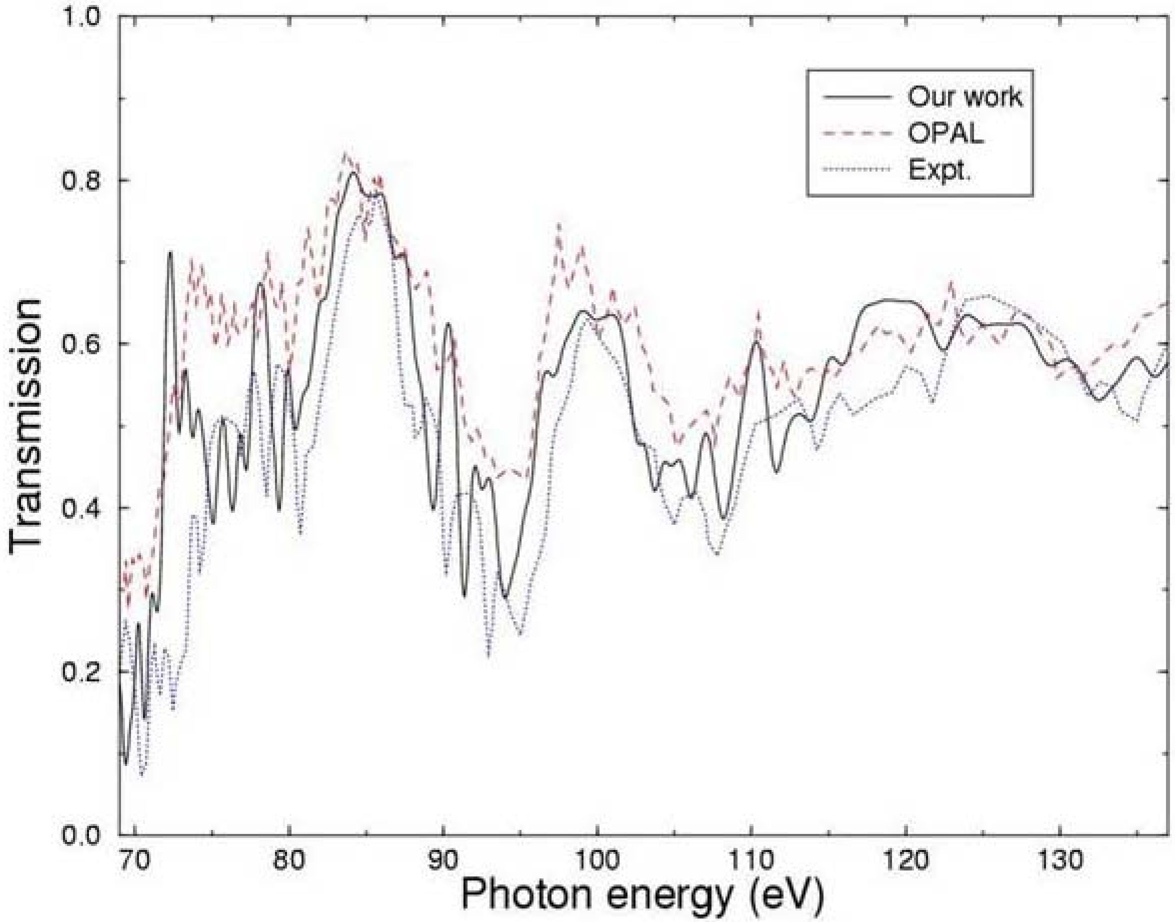

Phys. Rev. E 68, 066401 (2003) .

4. CI for the line position and strength:

FeVIII core-valence correlation for the energy levels and oscillator strength of a open 3d shell ion

Oscillator strength of $3s^2 3p^6 3d$---$3s^2 3p^5 3d^2$ transition array:

1---$3s^2 3p^6 3d\ ^2D_{3/2}$

2--- $3s^2 3p^6 3d\ ^2D_{5/2}$

3--- $3s^2 3p^5 3d^2 (^3F)\ ^2F^o_{5/2}$

4---$3s^2 3p^5 3d^2 (^3P)\ ^2P^o_{1/2}$

5---$3s^2 3p^5 3d^2 (^3F)\ ^2D^o_{3/2}$

6---$3s^2 3p^5 3d^2 (^3F)\ ^2F^o_{7/2}$

7---$3s^2 3p^5 3d^2 (^3P)\ ^2P^o_{3/2}$

8---$3s^2 3p^5 3d^2 (^3F)\ ^2D^o_{5/2}$

J. Phys. B 36, 3457 (2003) .

4. CI for the line position and strength:

FeVIII core-valence correlation for the energy levels and oscillator strength of a open 3d shell ion (continued）

Five sets of calculations are carried out to show the influence of the CI on the oscillator strength with Fe VIII as an example：

A: One-configuration Hartree-Fock (interactions within a configuration are considered)

B: $3s^23p^6nl$, $3s^23p^53dnl$, $3s^23p^5nln'l'$, $3s3p^63dnl$

C: $B+3p^2$---$3d^2$

D: $C+3p^3$---$3d^3$

E: $D+3p^m$---$3d^m$ (m=4,5,6)

4. CI for the line position and strength:

FeVIII core-valence correlation for the energy levels and oscillator strength of a open 3d shell ion (continued)

The gf in $3s^23p^63d$---$3s^23p^53d^2$ transition array:

Transitions	A	B	C	D	E	Bhatia
1-3	4.909	3.787	2.971	2.897	2.872	5.147
1-4	2.698	2.362	2.154	2.046	2.043	2.484
1-5	6.036	6.123	4.775	4.622	4.570	6.027
2-6	7.095	5.437	4.249	4.167	4.132	5.279
2-7	4.875	4.270	3.893	3.686	3.679	4.495
2-8	9.361	9.503	7.408	7.171	7.090	9.719

J. Phys. B 36, 3457 (2003) .

4. CI for the line position and strength:

FeVIII core-valence correlation for the energy levels and oscillator strength of a open 3d shell ion (continued)

FeVIII, $3s^23p^63d$---$3s^23p^53d^2$ transition array

D=0.01g/cm^3
T=20 eV

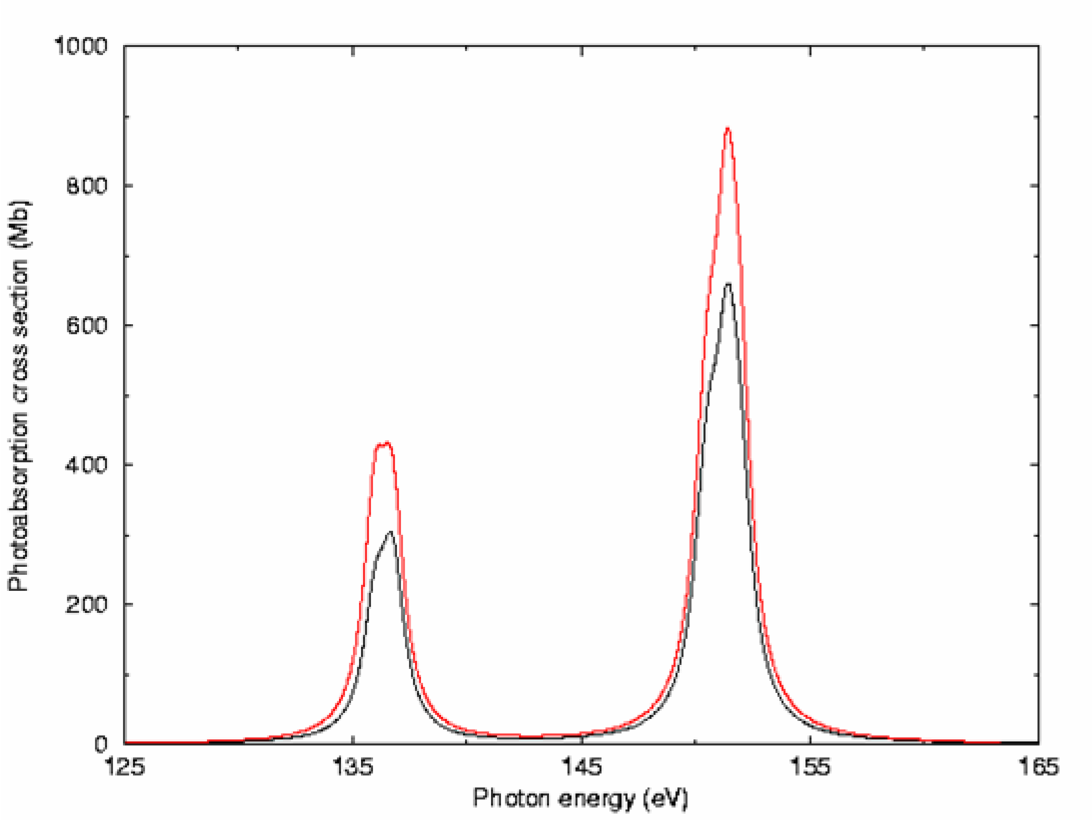

4. CI for the line position and strength:

The transmission spectrum of Fe plasma in the 2p-3d excitation region

C. Chenais-Popovics *et al.*, Astrophys. J., Suppl. Ser. 127, 275(2000)

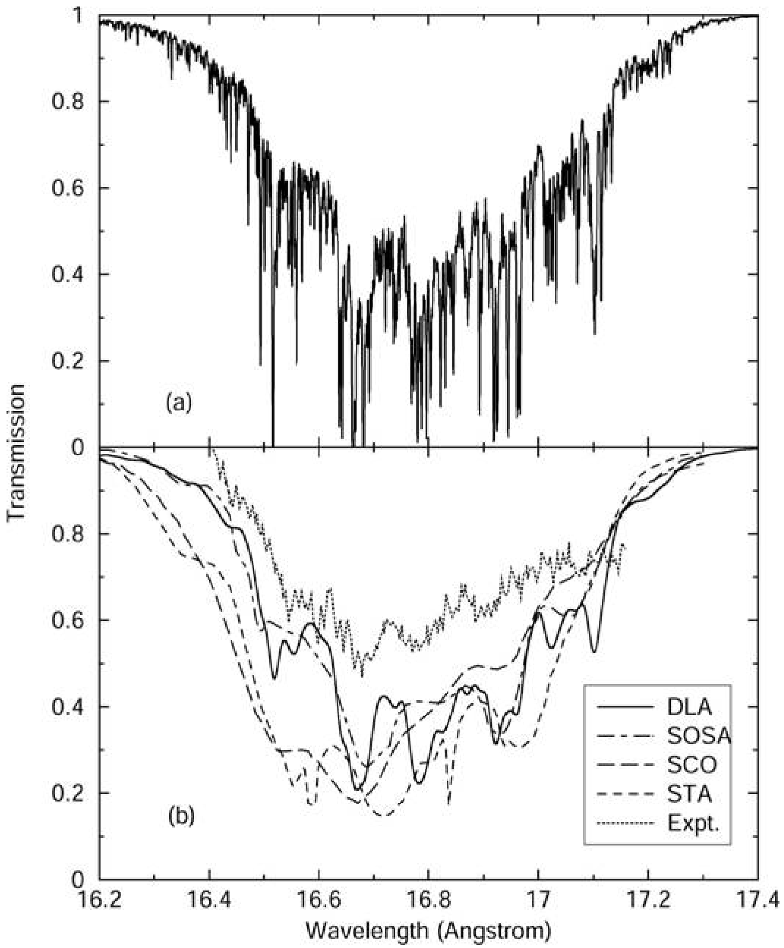

A constant autoionization width for all lines

4. CI for the line position and strength:

The transmission spectrum of Fe plasma in the 2p-3d excitation region (continued)

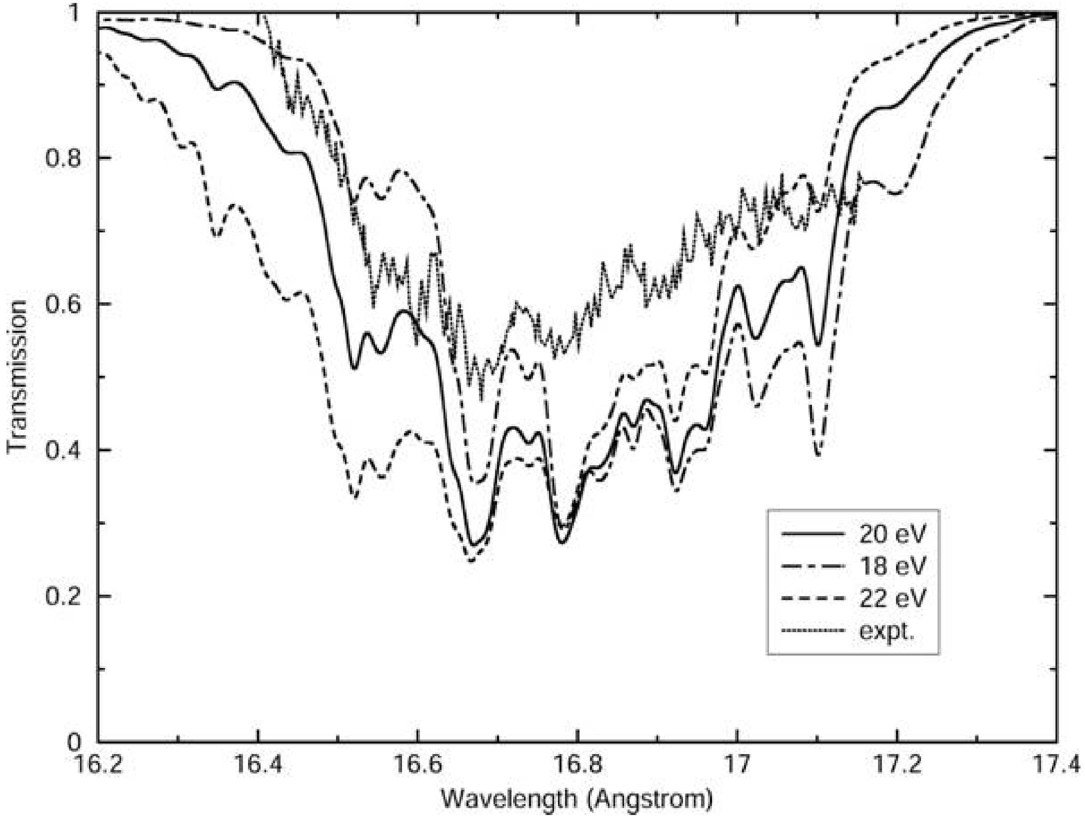

Phys. Rev. E **70**, 027401 (2004)

Autoionization width is calculated line by line

4. CI for the line position and strength:

The transmission spectrum of Fe plasma in the 2p-3d excitation region (continued)

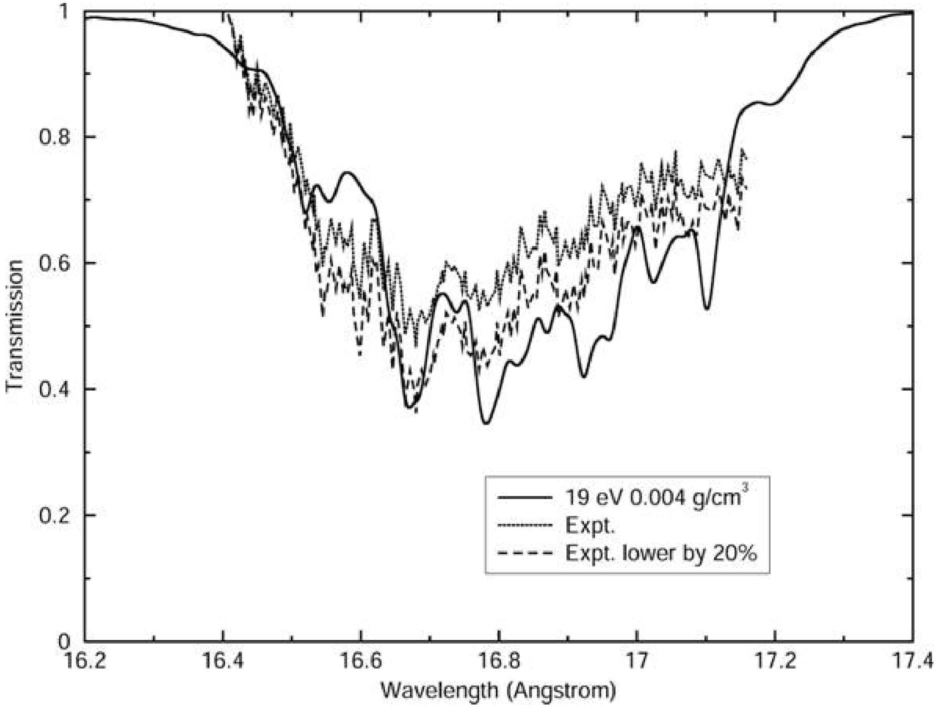

CI is taken into account resulting in a 20% reduction of the absorption strength

Phys. Rev. E 70, 027401(2004)

4.Iron opacity: correlation induced changes

Fe^{4+}-Fe^{9+}

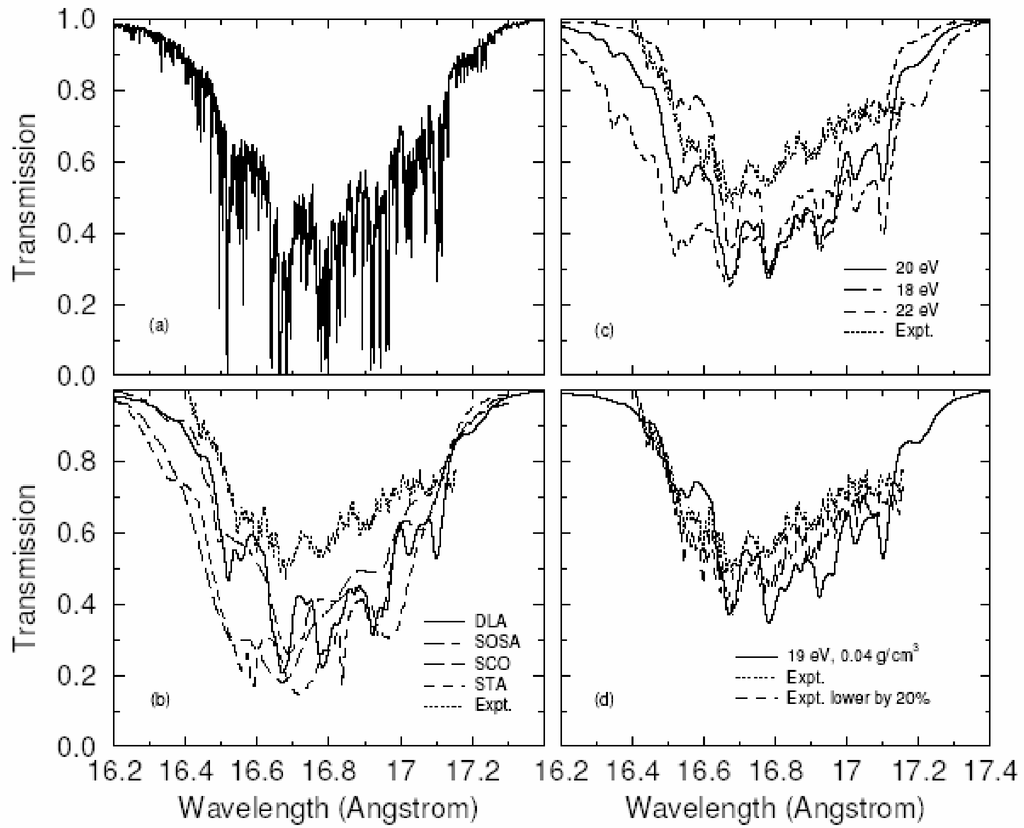

FIGURE 4. Transmission calculated as a function of wavelength at a temperature of 20 eV and a density of 0.004 g/cm^3. The autoionization width is taken to be 140 meV for all lines. Instrumental broadening (a) not included and (b) included. The insert (c), transmission at temperatures of 18, 20, and 22 eV with autoionization widths calculated by FAC for all lines. Insert (d), transmission at a temperature of 19 eV obtained by further considering the configuration interaction effect.

Phys. Rev. E 70, 027401(2004)

5. Br opacity

Exp:J. E. Bailey *et al.*, JQSRT 81, 31 (2003)

- T=37 eV， ρ =0.025 g/cm^3

Br^{7+}-Br^{12+}

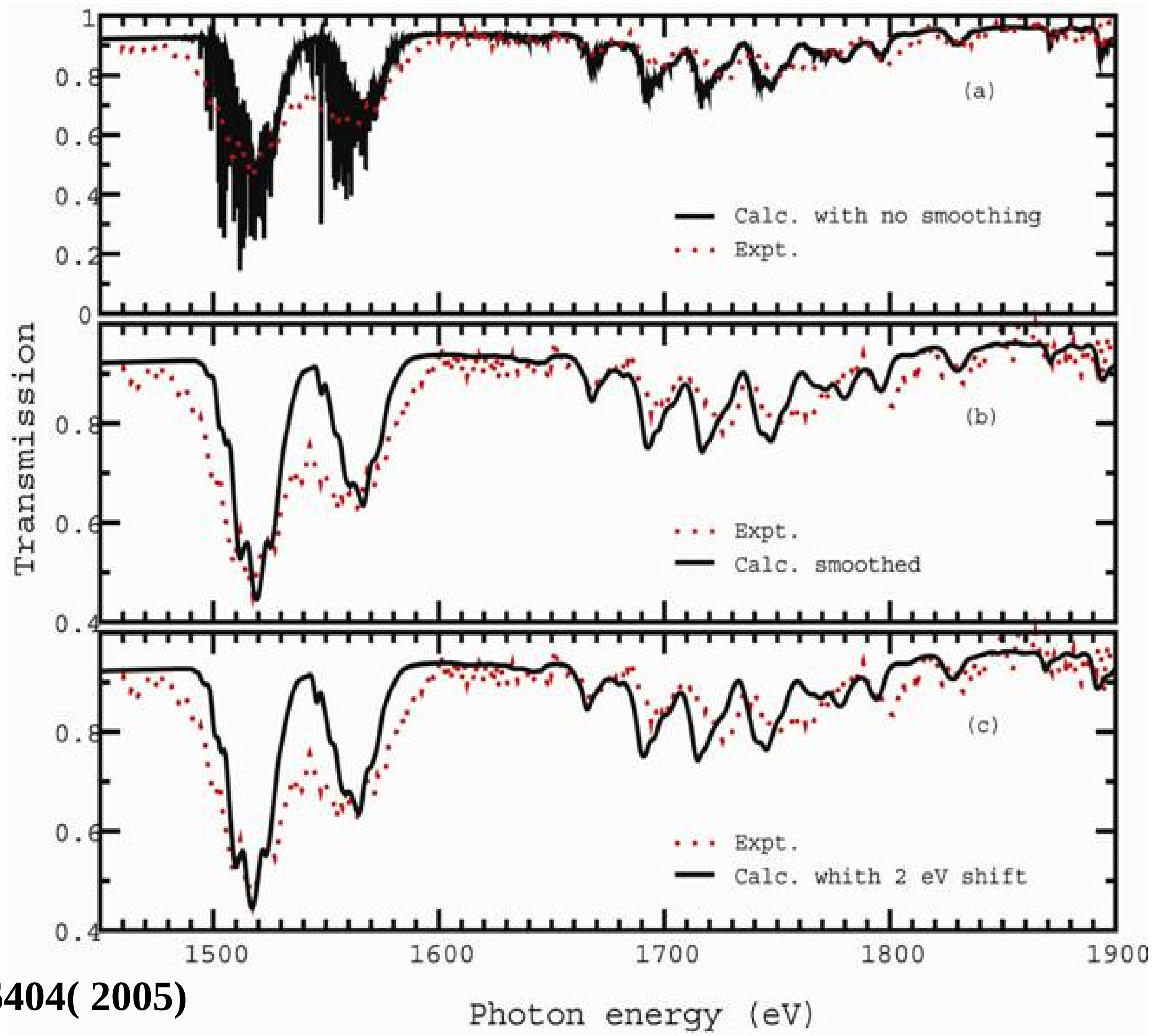

Phys. Rev. E 72, 016404(2005)

5. Absorption of Br ions

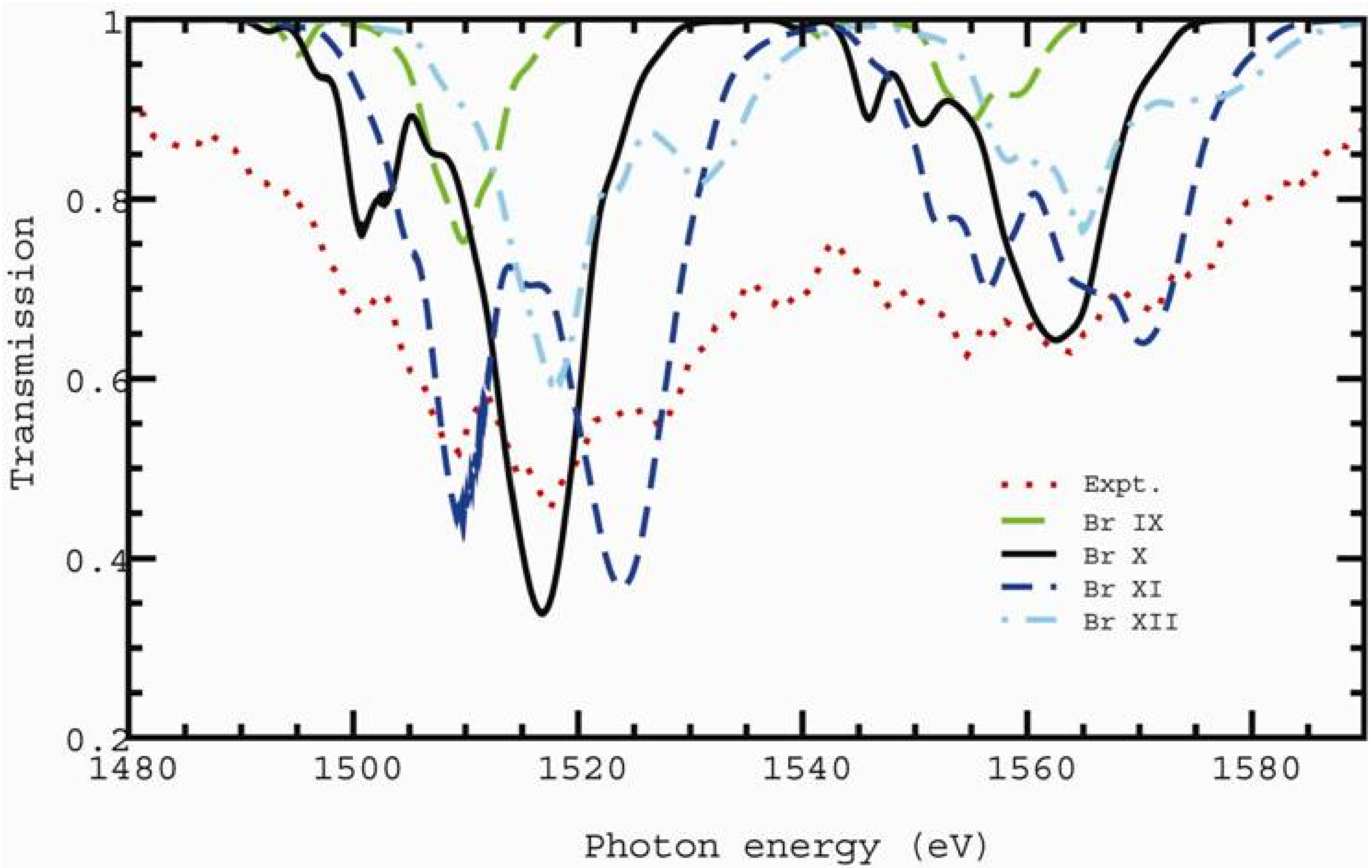

5. Temperature dependent

- 0.025g/cm^3
- (a)、(b)、(c) 36、37 and 38 V

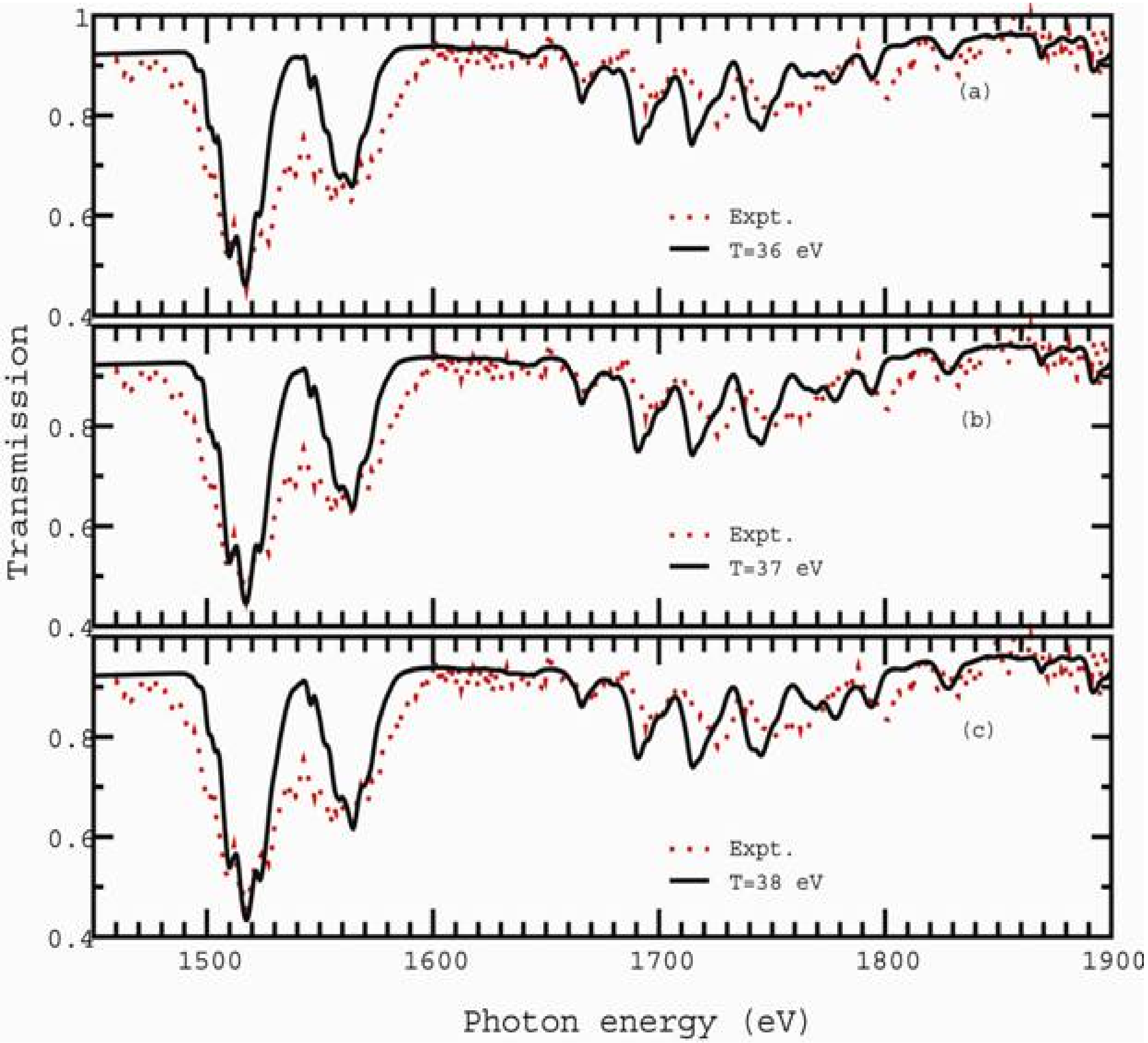

5. Density dependence

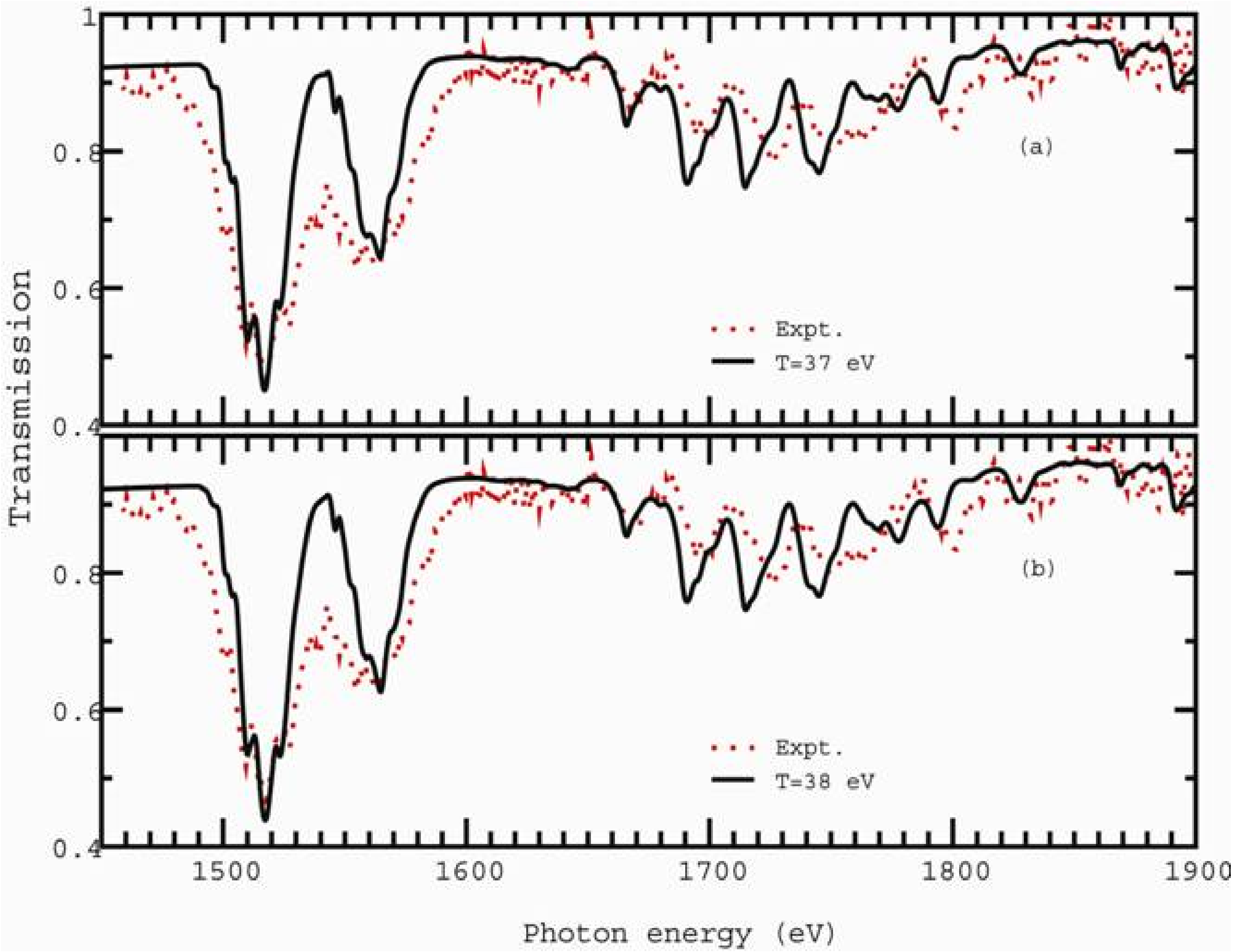

- 0.03g/cm^3， 37 and 38eV

5. Comparison between different theories

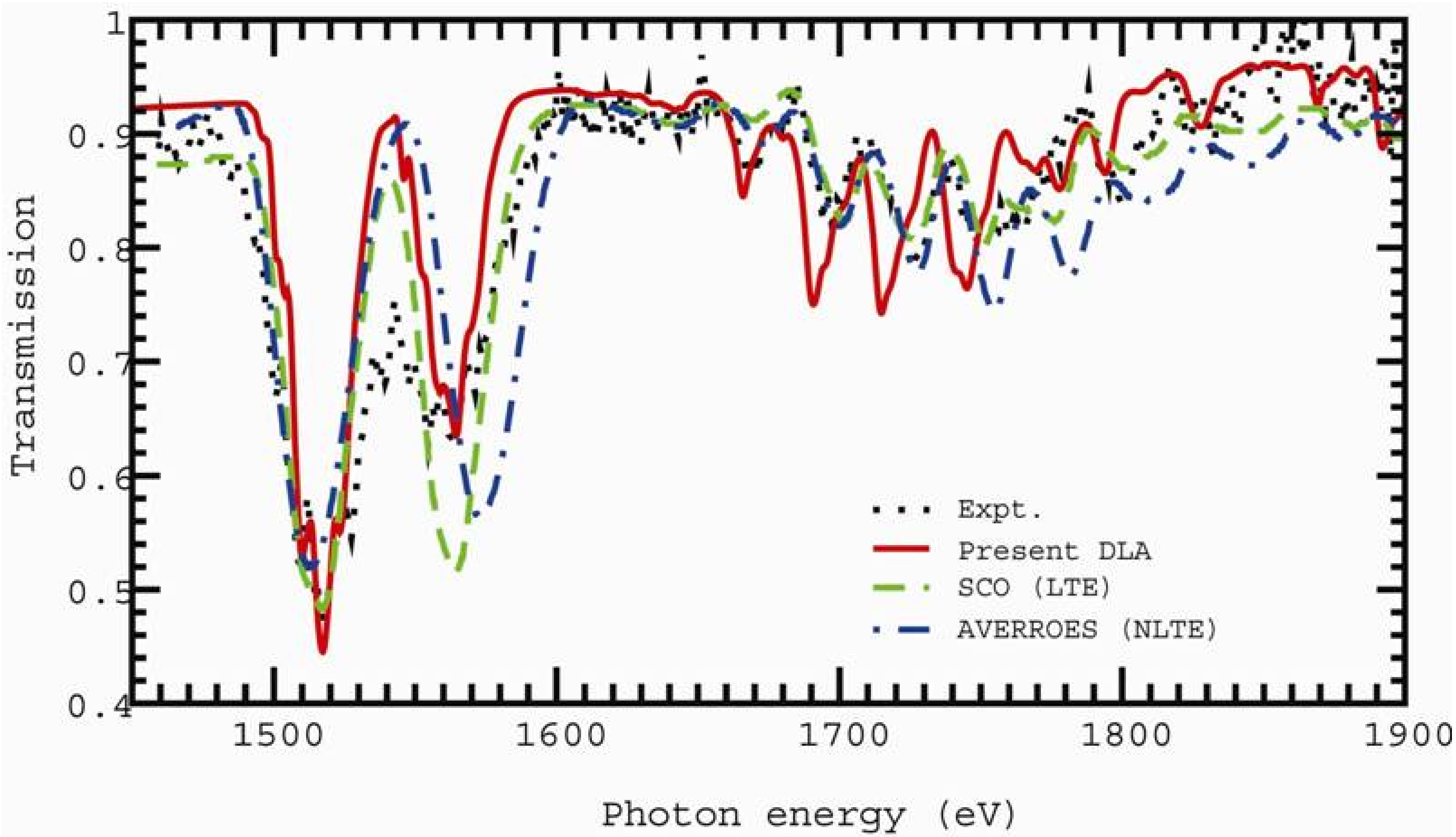

6. Au opacity at 22.5 eV and 0.007 g/cm^3

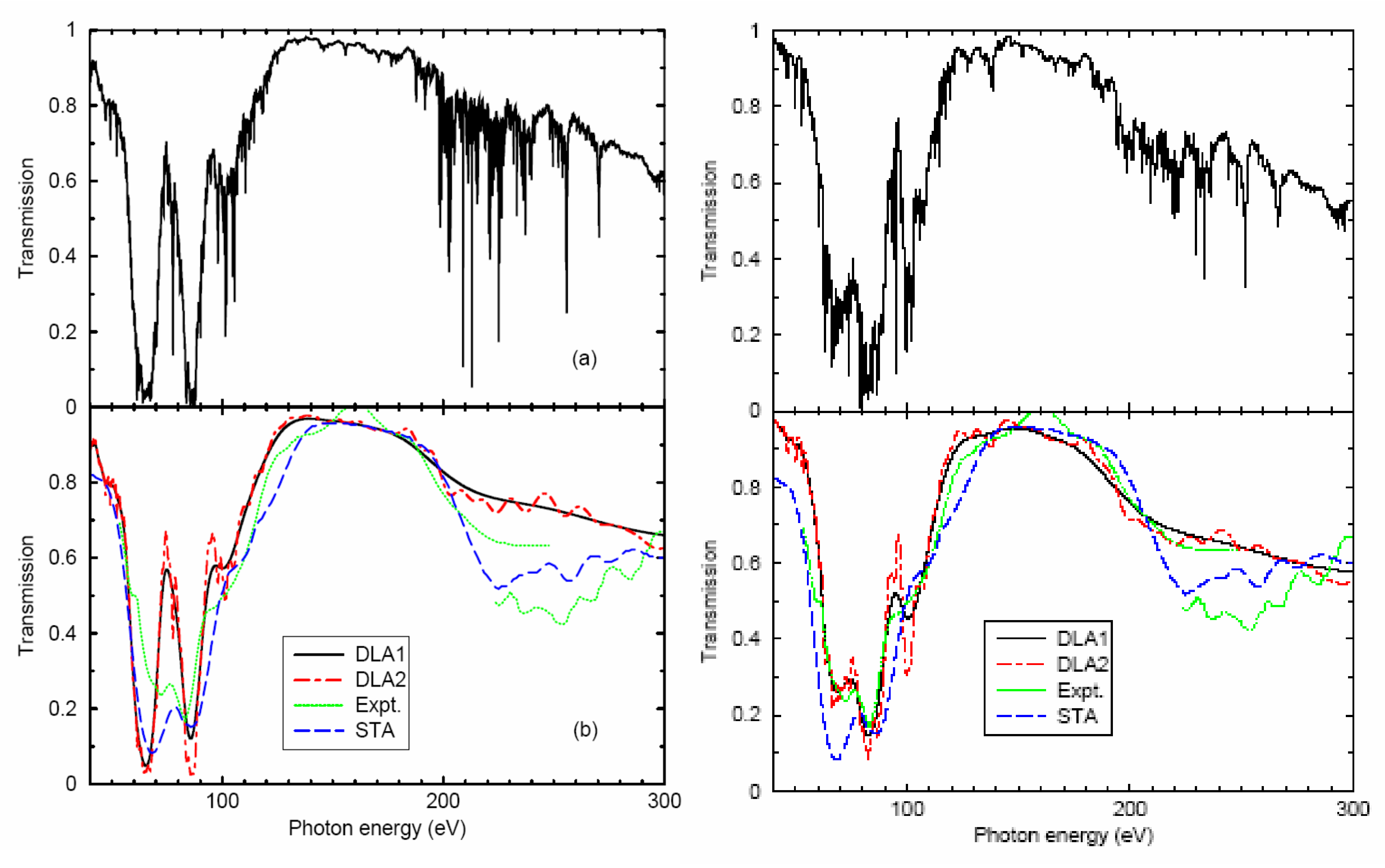

Phys. Rev. E 74, 025401(R)(2006)

5. core-valence correlation effects

- Au^{11+}， $[Kr]4s^2 4p^6 4d^{10} 4f^{14} 5s^2 5p^6$
- A： one-configuration Dirac-Fock
- B： one electron excited
- C： B plus double electron excited
- D： C plus three electron excited

- for transition arrays $5p^6$---$5p^{-1}5d$, $5p^6$---$4f^{-1}5d$

Lower	Upper	A	B	C	D
$5p^6$	$(5p^{-1}_{3/2}5d_{5/2})_1$	2.055	1.897	1.476	1.611
$5p^6$	$(5p^{-1}_{1/2}5d_{3/2})_1$	6.555	5.071	2.534	2.666
$5p^6$	$(4f^{-1}_{7/2}5d_{5/2})_1$	0.021	0.558	0.041	0.036
$5p^6$	$(4f^{-1}_{5/2}5d_{5/2})_1$	0.434	0.169	0.135	0.176
$5p^6$	$(4f^{-1}_{7/2}5d_{5/2})_1$	0.695	2.497	3.297	2.980

6. CI effects

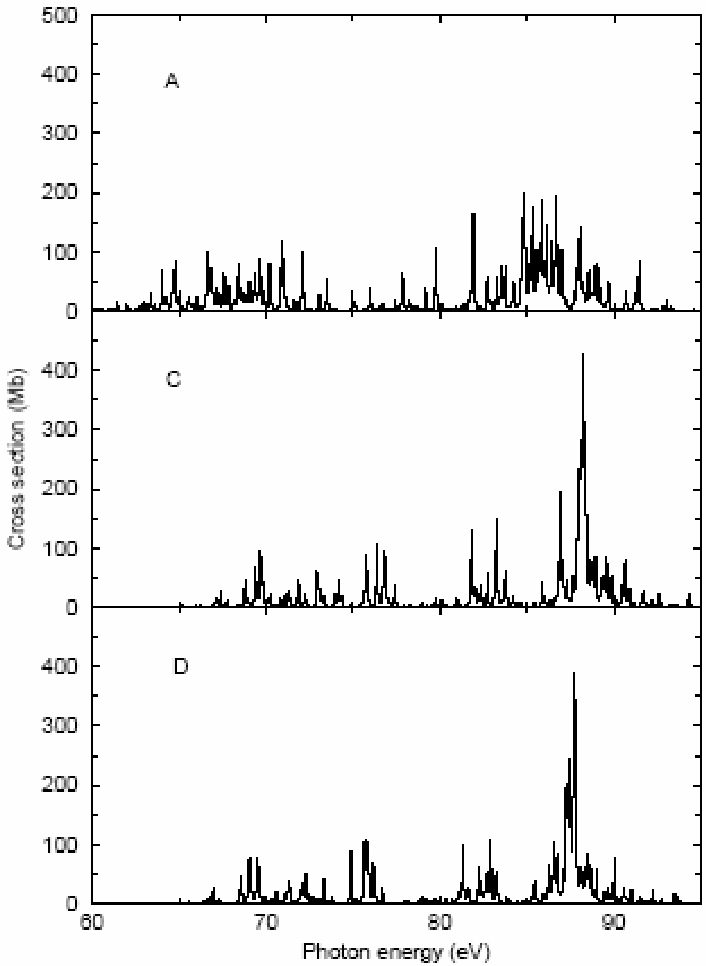

$5p^55d$ --- $5p^45d^2$

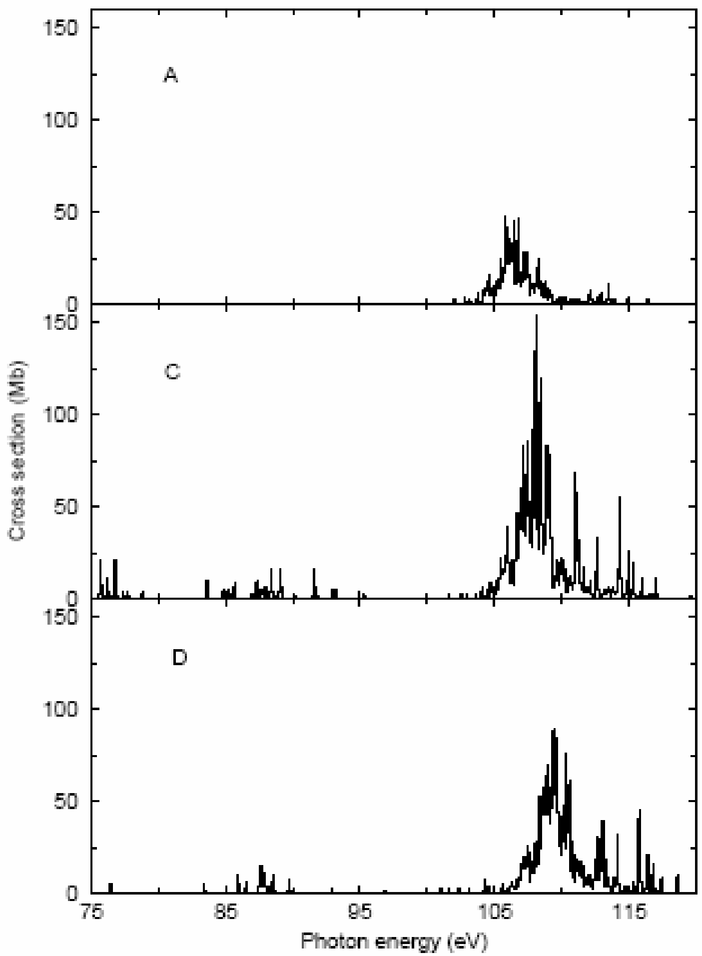

$5p^55d$ --- $4f^{13}5p^55d^2$

6. Au opacity at 22.5 eV and 0.007 g/cm^3

Exp:Eidmann *et al*. Europhys.Lett. **44**, 459(1998).

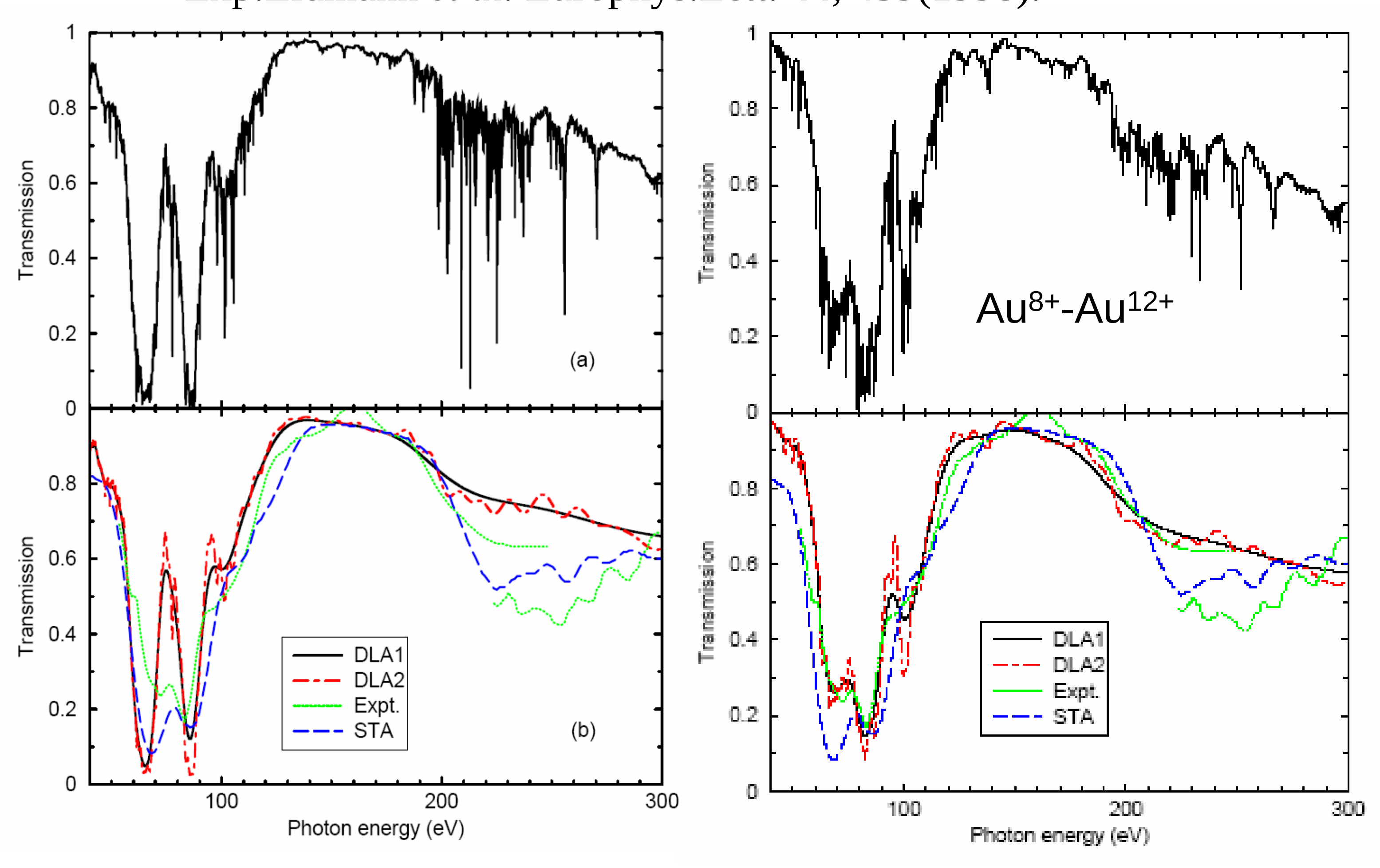

Theory: Phys. Rev. E 74, 025401(R)(2006)

Density effects on the structures and processes

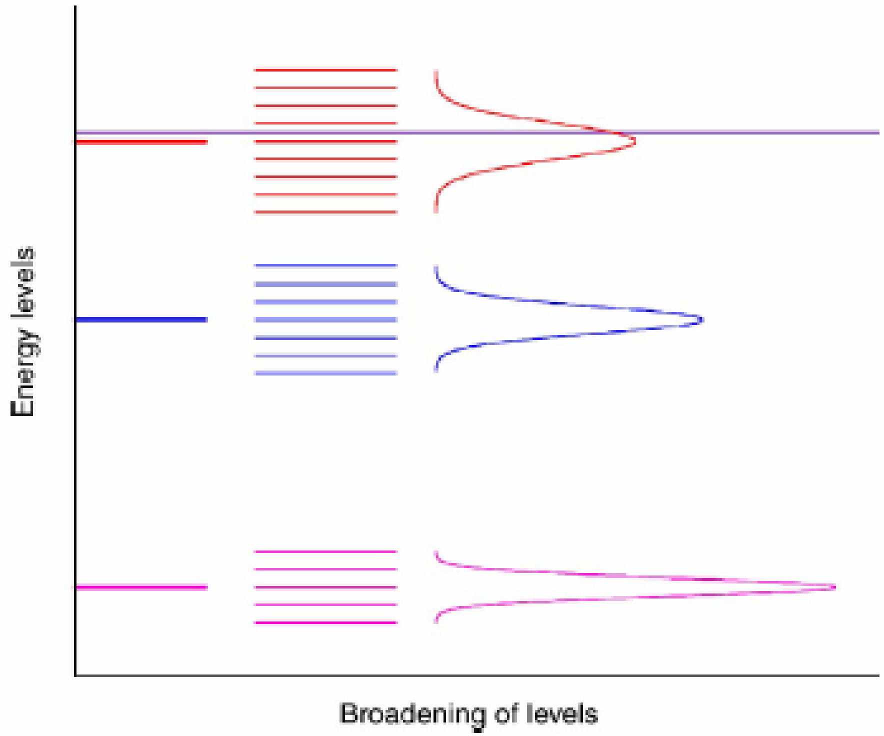

FIG. 1. Splits of bound state energy levels into many sublevels in plasma, which are described approximately by a Gaussian distributed density of states.

PHYSICS OF PLASMAS 13, 093301 (2006)

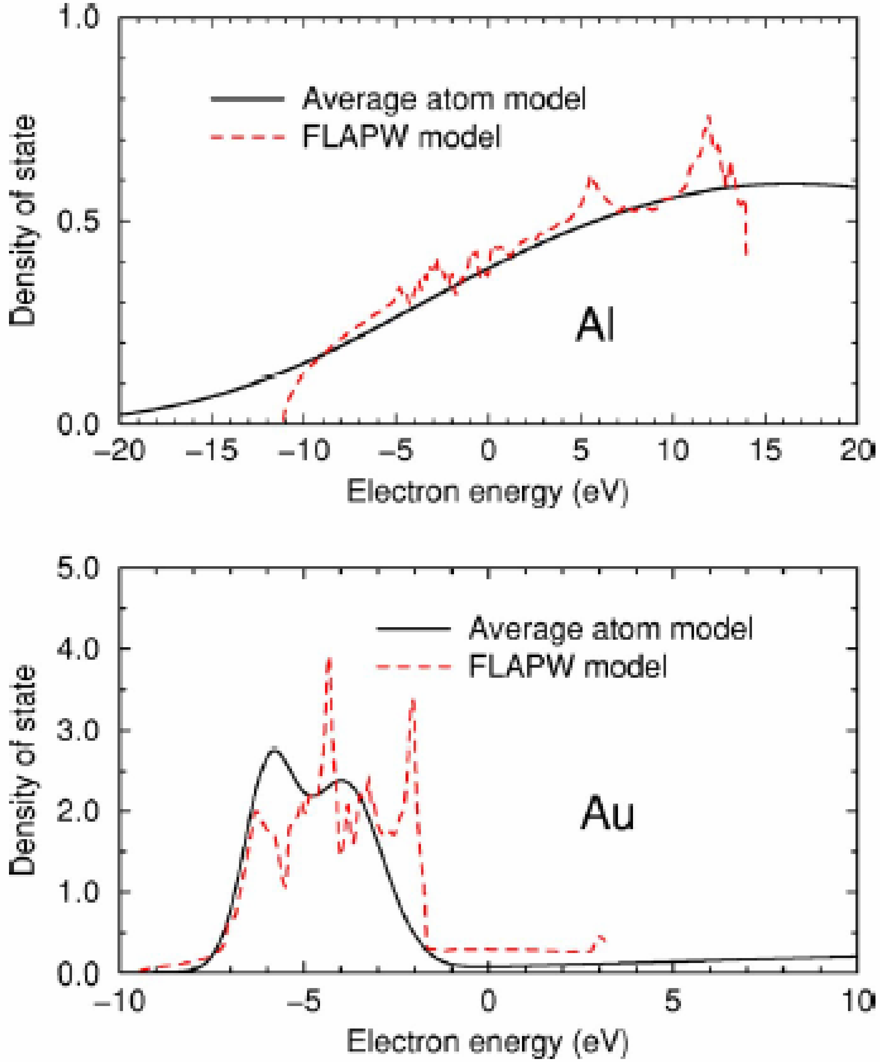

FIG. 2. Density of state across the Fermi level: comparisons between the present AA model and the FLAPW model for Al and Au at solid density.

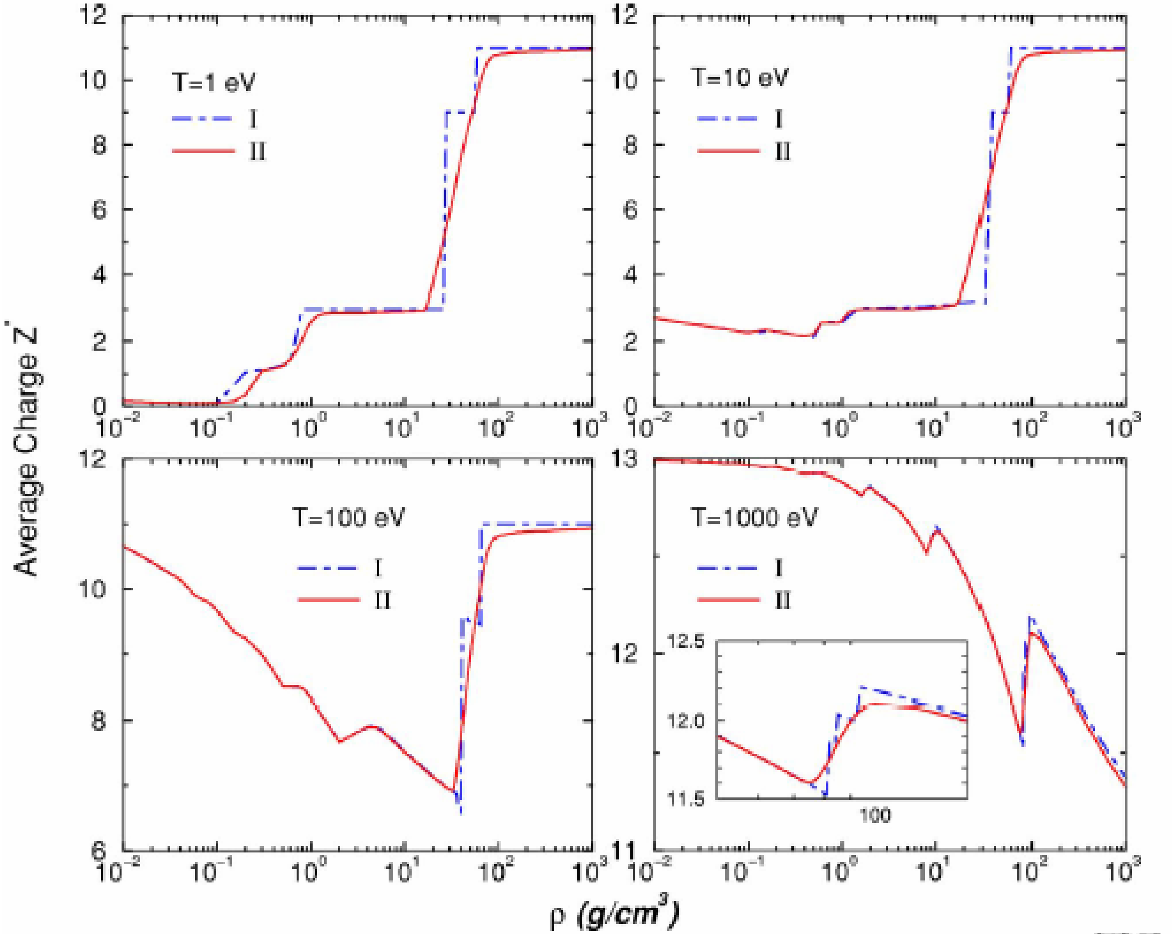

FIG. 3. Density dependence of the average ionization degree of Al at 1, 10, 100, and 1000 eV. The results without and with the level broadening are labeled as I and II, respectively.

PHYSICS OF PLASMAS 13, 093301 (2006)

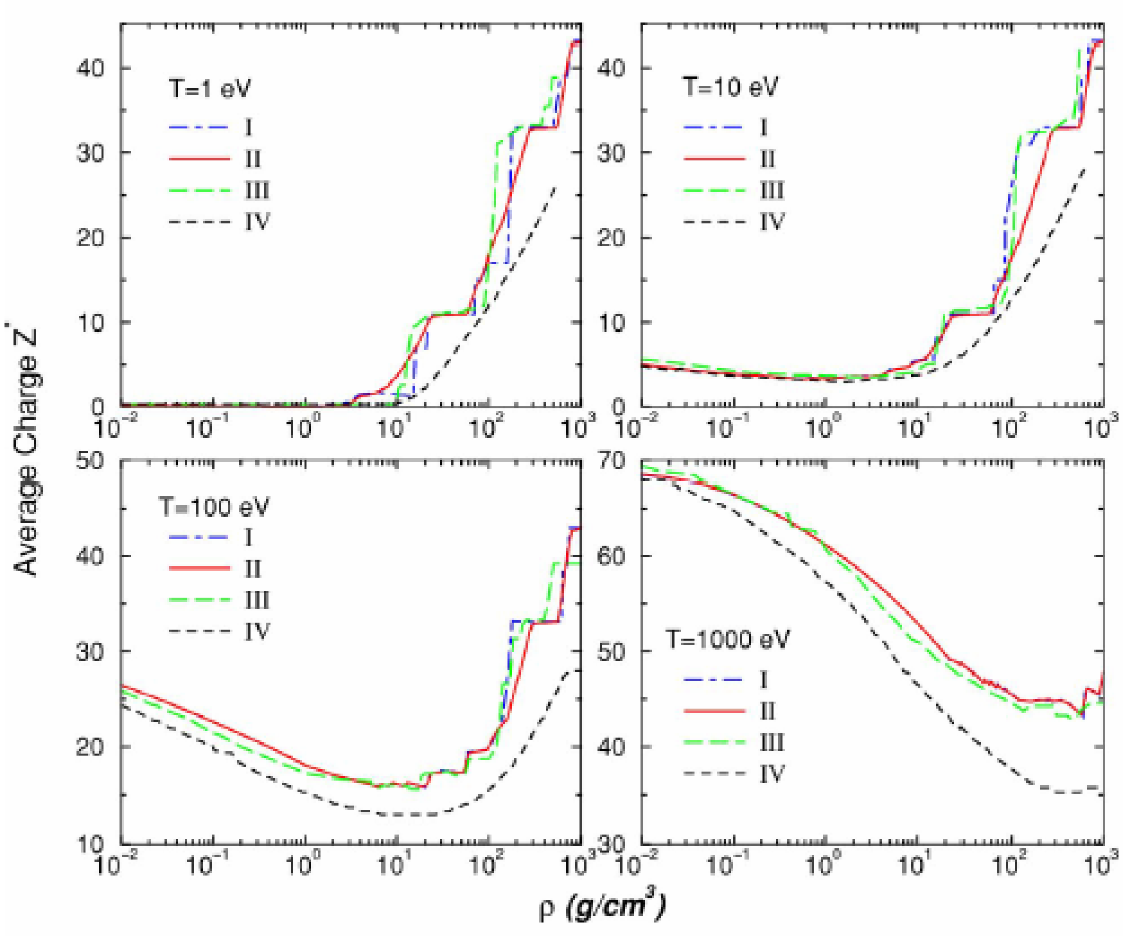

FIG. 4. Density dependence of the average ionization degree of Au at 1, 10, 100, and 1000 eV. The results of the present AA model are labeled in the same way as in Fig. 3. Comparison is made between the present result and the STA result of Ref. 13, for which III and IV are used to distinguish the data without and with the shape resonant orbitals.

PHYSICS OF PLASMAS 13, 093301 (2006)

Conclusions

I. A detailed line treatment is essential for a quantitative comparison between theory and experiment;

II. High accurate atomic data is required for the predictions of both the position and strength of the spectral fine structures;

III. The combining influence of electronic correlation and relativistic effects on the atomic data and the calculated opacity;

IV. Methods for effective and large scale parallel calculations of the atomic data;

V. The density influences on the energy levels and cross sections of the ions in plasma.

This work is supported by the National Natural Science Foundation of China, China ICF committee, and CRAAMD.

Thank you for your attention